



HAL
open science

Analyzing diversification dynamics using barcoding data: the case of an obligate mycorrhizal symbiont

Benoît Perez-Lamarque, Maarja Öpik, Odile Maliet, Ana Afonso Silva, Marc-André Selosse, Florent Martos, Hélène Morlon

► **To cite this version:**

Benoît Perez-Lamarque, Maarja Öpik, Odile Maliet, Ana Afonso Silva, Marc-André Selosse, et al.. Analyzing diversification dynamics using barcoding data: the case of an obligate mycorrhizal symbiont. *Molecular Ecology*, 2022, 10.1111/mec.16478 . hal-03650682

HAL Id: hal-03650682

<https://hal.sorbonne-universite.fr/hal-03650682v1>

Submitted on 25 Apr 2022

HAL is a multi-disciplinary open access archive for the deposit and dissemination of scientific research documents, whether they are published or not. The documents may come from teaching and research institutions in France or abroad, or from public or private research centers.

L'archive ouverte pluridisciplinaire **HAL**, est destinée au dépôt et à la diffusion de documents scientifiques de niveau recherche, publiés ou non, émanant des établissements d'enseignement et de recherche français ou étrangers, des laboratoires publics ou privés.

1 **Analyzing diversification dynamics using barcoding data:**
2 **the case of an obligate mycorrhizal symbiont**

3
4 Benoît Perez-Lamarque ^{1,2*}, Maarja Öpik ³, Odile Maliet ¹, Ana C. Afonso Silva ¹, Marc-
5 André Selosse ^{2,4}, Florent Martos ², and Hélène Morlon ¹

6
7
8 ¹ *Institut de biologie de l'École normale supérieure (IBENS), École normale supérieure, CNRS,*
9 *INSERM, Université PSL, 46 rue d'Ulm, 75 005 Paris, France*

10 ² *Institut de Systématique, Évolution, Biodiversité (ISYEB), Muséum national d'histoire naturelle,*
11 *CNRS, Sorbonne Université, EPHE, UA, CP39, 57 rue Cuvier 75 005 Paris, France*

12 ³ *University of Tartu, 40 Lai Street, 51 005 Tartu, Estonia*

13 ⁴ *Department of Plant Taxonomy and Nature Conservation, University of Gdansk, Wita Stwosza*
14 *59, 80-308 Gdansk, Poland*

15
16 * *corresponding author: benoit.perez@ens.psl.eu; ORCID: 0000-0001-7112-7197*

17

18 ***Abstract:***

19

20 Analyzing diversification dynamics is key to understanding the past evolutionary history
21 of clades that led to present-day biodiversity patterns. While such analyses are widespread
22 in well-characterized groups of species, they are much more challenging in groups which
23 diversity is mostly known through molecular techniques. Here, we use the largest global
24 database on the small subunit (SSU) rRNA gene of Glomeromycotina, a subphylum of
25 microscopic arbuscular mycorrhizal fungi that provide mineral nutrients to most land
26 plants by forming one of the oldest terrestrial symbioses, to analyze the diversification
27 dynamics of this clade in the past 500 million years (Myr). We perform a range of sensitivity
28 analyses and simulations to control for potential biases linked to the nature of the data. We
29 find that Glomeromycotina tend to have low speciation rates compared to other
30 eukaryotes. After a peak of speciations between 200 and 100 Myr ago, they experienced an
31 important decline in speciation rates toward the present. Such a decline could be at least
32 partially related to a shrinking of their mycorrhizal niches and to their limited ability to
33 colonize new niches. Our analyses identify patterns of diversification in a group of obligate
34 symbionts of major ecological and evolutionary importance and illustrate that short
35 molecular markers combined with intensive sensitivity analyses can be useful for studying
36 diversification dynamics in microbial groups.

37

38 Key words: microbial diversification, arbuscular mycorrhiza, obligate symbiosis,
39 ecological niche, macroevolution, fungi.

40 ***Introduction:***

41

42 Understanding past dynamics of speciation and extinction, as well as the abiotic and
43 biotic factors that modulate the frequency of speciation and extinction events (i.e.
44 diversification rates) is key to understanding the historical processes that shaped present-
45 day biodiversity patterns (Barnosky, 2001; Condamine, Rolland, Höhna, Sperling, &
46 Sanmartín, 2018; Morlon, 2014; Varga et al., 2019) (Barnosky, 2001; Benton, 2009; Chomicki,
47 Kiers, & Renner, 2020; Clarke & Gaston, 2006). While phylogenetic analyses of
48 diversification are widespread in well-characterized groups of species, such as animals and
49 plants (Givnish et al., 2015; Magallón & Sanderson, 2001; Rolland, Condamine, Jiguet, &
50 Morlon, 2014; Upham, Esselstyn, & Jetz, 2019), they are much more challenging in groups
51 which diversity is mostly known through environmental DNA sequences and molecular
52 techniques. In particular, the characterization of poorly cultivable microbial groups such
53 as most bacteria and fungi is often limited to metabarcoding techniques, which consist in
54 the specific amplification and sequencing of a short DNA region (Taberlet, Bonin, Zinger,
55 & Coissac, 2018). On the one hand, these data often render species delineation,
56 phylogenetic reconstruction, and the estimation of global scale diversity highly uncertain,
57 which all affect the phylogenetic inference of diversification dynamics (Lekberg et al., 2018;
58 Moen & Morlon, 2014). On the other hand, it is possible to assess the robustness of
59 phylogenetic diversification analyses to data uncertainty. Given the current limitations of
60 sequencing technologies and the nature of the molecular data available for most microbial
61 groups, using metabarcoding data and performing thorough robustness analyses is one of
62 the only (if not the only) possible approach to analyze their diversification dynamics
63 (Davison et al., 2015; Lewitus, Bittner, Malviya, Bowler, & Morlon, 2018; Louca et al., 2018).

64

65 Here we analyze the diversification dynamics of arbuscular mycorrhizal fungi from
66 the subphylum Glomeromycotina. These fungi are obligate symbionts that have been
67 referred to as an “evolutionary cul-de-sac, albeit an enormously successful one” (Malloch,
68 1987; Morton, 1990). This alludes to their ecological success despite limited morphological

69 and species diversities: they associate with the roots of >80% of land plants, where they
70 provide mineral resources in exchange for photosynthates (Smith & Read, 2008). Present
71 in most terrestrial ecosystems, Glomeromycotina play key roles in plant protection,
72 nutrient cycling, and ecosystem processes (van der Heijden, Martin, Selosse, & Sanders,
73 2015). Fossil evidence and molecular phylogenies suggest that Glomeromycotina
74 contributed to the emergence of land plants (Feijen, Vos, Nuytinck, & Merckx, 2018; Field,
75 Pressel, Duckett, Rimington, & Bidartondo, 2015; Selosse & Le Tacon, 1998; Strullu-
76 Derrien, Selosse, Kenrick, & Martin, 2018) and coevolved with them for more than 400
77 million years (Myr)(Lutzoni et al., 2018; Simon, Bousquet, Lévesque, & Lalonde, 1993;
78 Strullu-Derrien et al., 2018).

79

80 Glomeromycotina are microscopic soil- and root-dwelling fungi that are hard to
81 differentiate based on morphology and difficult to cultivate without host plant. Although
82 their classical taxonomy is mostly based on the characters of spores and root colonization
83 (Smith & Read, 2008; Stürmer, 2012), Glomeromycotina species delineation has greatly
84 benefited from DNA sequencing (Krüger, Krüger, Walker, Stockinger, & Schüßler, 2012).
85 Experts have defined “virtual taxa” (VT) based on a minimal 97% similarity of a region of
86 the 18S small subunit (SSU) rRNA gene and monophyly criteria (Öpik, Davison, Moora, &
87 Zobel, 2014; Öpik et al., 2010). As for many other pragmatic species delineation criteria, VT
88 have rarely been tested for their biological relevance (Powell, Monaghan, Öpik, & Rillig,
89 2011), and a consensual system of Glomeromycotina classification is still lacking (Bruns,
90 Corradi, Redecker, Taylor, & Öpik, 2018). Besides the rDNA region, Glomeromycotina
91 remain poorly known genetically: other gene sequences are available for only a few species
92 (James et al., 2006; Lutzoni et al., 2018) and less than 30 complete genomes are currently
93 available (Venice et al., 2020).

94

95 Hence, despite the ecological ubiquity and evolutionary importance of
96 Glomeromycotina, large-scale patterns of their diversification dynamics, as well as the
97 factors that correlate with these dynamics, remain poorly known. A previous dated

98 phylogenetic tree of VT found that many speciation events occurred after the last major
99 continental reconfiguration around 100 Myr ago (Davison et al., 2015), suggesting the
100 radiation of Glomeromycotina is not linked to vicariant speciation during this geological
101 event. Indeed, vicariant speciation might only play a minor role in Glomeromycotina
102 diversification, as these organisms have spores that disperse efficiently, promoting gene
103 flow (Bueno & Moora, 2019; Correia, Heleno, da Silva, Costa, & Rodríguez-Echeverría,
104 2019; Egan, Li, & Klironomos, 2014). Based on the diversity and abundance of
105 Glomeromycotina in tropical grasslands (Read, 1991), it has been suggested (but never
106 tested) that these habitats are diversification hotspots for Glomeromycotina (Pärtel et al.,
107 2017). In this case, the pace of Glomeromycotina diversification through time could be
108 tightly linked to changes in the total area of tropical grasslands. Finally, Glomeromycotina
109 are currently obligate symbionts and their evolutionary history could thus have been
110 largely influenced by their interactions with their host plants (Lutzoni et al., 2018; Sauquet
111 & Magallón, 2018; Zanne et al., 2014). Over the last 400 Myr, land plants have experienced
112 massive extinctions and radiations (Cleal & Cascales-Miñana, 2014; Zanne et al., 2014),
113 adaptations to various ecosystems (Bredenkamp, Spada, & Kazmierczak, 2002; Brundrett
114 & Tedersoo, 2018), and associations with different soil microorganisms (Werner et al., 2018;
115 Werner, Cornwell, Sprent, Kattge, & Kiers, 2014). All these events could have influenced
116 the diversification dynamics of Glomeromycotina, although their relative generalism
117 (Perez-Lamarque, Selosse, Öpik, Morlon, & Martos, 2020; Sanders, 2003; van der Heijden
118 et al., 2015) could buffer this influence.

119

120 We aim to characterize the pace of Glomeromycotina diversification in the last 500
121 Myr and to test the association between diversification rates and a variety of biotic and
122 abiotic factors. We begin by reconstructing several thoroughly sampled phylogenetic trees
123 of Glomeromycotina, considering several criteria of species delineations and uncertainty
124 in phylogenetic reconstructions. We combine this phylogenetic data with
125 paleoenvironmental data and data of current Glomeromycotina geographic distributions,
126 ecological traits, interaction with host plants, and genetic diversity. Finally, we apply a

127 series of birth-death models of cladogenesis to answer specific questions and test
128 hypotheses related to Glomeromycotina diversification: (i) how often do speciation events
129 occur? (ii) were speciation rates relatively constant, or were they higher during specific
130 periods of evolutionary history? and do speciation rates decline through time, as observed
131 for many macroorganisms (Moen & Morlon, 2014)? (iii) are speciation rates positively
132 correlated with past temperature, CO₂ concentration, and/or land plant diversity? (iv) are
133 present-day speciation rates correlated with geographic distribution, spore size (itself often
134 inversely related to dispersal capacity, Nathan et al., 2008), degree of specialization toward
135 plant species, and genetic diversity? For each of these questions, we thoroughly assess the
136 robustness of our results to uncertainty in the data.

137

138 **Material & methods:**

139

140 **Virtual taxa phylogenetic reconstruction:**

141

142 We downloaded the Glomeromycotina SSU rRNA gene sequences from MaarjAM,
143 the largest global database of Glomeromycotina gene sequences updated in June 2019
144 (Öpik et al., 2010). We reconstructed several Bayesian phylogenetic trees of the 384 *virtual*
145 *taxa* (VT) from the corresponding representative sequences available in the MaarjAM
146 database (Supplementary Methods 1). We used the full length (1,700 base pairs) SSU rRNA
147 gene sequences from (Rimington et al., 2018) to better align the VT sequences using MAFFT
148 (Kato & Standley, 2013). We selected the 520 base pair central variable region of the VT
149 aligned sequences and performed a Bayesian phylogenetic reconstruction using BEAST2
150 (Bouckaert et al., 2014). We set the crown root age at 505 Myr (Davison et al., 2015), which
151 is coherent with fossil data and previous dated molecular phylogenies (Lutzoni et al., 2018;
152 Strullu-Derrien et al., 2018). We also used the youngest (437 Myr) and oldest (530 Myr)
153 crown age estimates from (Lutzoni et al., 2018) in diversification analyses that may be
154 particularly sensitive to absolute dates.

155

156 **Delineation into Evolutionary Units (EUs):**

157

158 We considered several ways to delineate Glomeromycotina species based on the
159 SSU rRNA gene. In addition to the VT species proxy, we delineated Glomeromycotina *de*
160 *novo* into evolutionary units (EUs) using a monophyly criterion and 5 different thresholds
161 of sequence similarity ranging from 97 to 99%. We gathered Glomeromycotina sequences
162 of the SSU rRNA gene from MaarjAM, mainly amplified by the primer pair NS31–AML2
163 (variable region) (Lee, Lee, & Young, 2008; Simon, Lalonde, & Bruns, 1992) (dataset 1,
164 Supplementary Table 1). There were 36,411 sequences corresponding to 27,728 haplotypes.
165 We first built a phylogenetic tree of these haplotypes and then applied to this tree our own
166 algorithm of EU delineation (R-package RPANDA (Morlon et al., 2016; R Core Team, 2020))

167 that traverses the tree from the root to the tips, at every node computes the average
168 similarity of all sequences descending from the node, and collapses the sequences into a
169 single EU if their sequence dissimilarity is lower than a given threshold (Supplementary
170 Methods 2). In other words, Glomeromycotina sequences are merged into the same EU if
171 they form a monophyletic clade and if they are on average more similar than the sequence
172 similarity threshold. Finally, we performed Bayesian phylogenetic reconstructions of the
173 EUs using BEAST2, using the same crown ages as above (Supplementary Methods 1).

174

175 **Coalescent-based species delineation analyses:**

176

177 Finally, we considered the Generalized Mixed Yule Coalescent method (GMYC)
178 (Fujisawa & Barraclough, 2013; Pons et al., 2006), a species delineation approach that does
179 not require specifying an arbitrary similarity threshold. GMYC estimates the time t in a
180 reconstructed calibrated tree that separates species diversification (Yule process – before t)
181 and intraspecific differentiation (coalescent process – after t). GMYC is too computationally
182 intensive to be applied to the 36,411 SSU sequences; we used it here on three clades of
183 manageable size (the family Claroideoglomeraceae; the order Diversisporales; and an
184 early-diverging clade composed of the orders Archaeosporales and Paraglomerales) to (i)
185 investigate whether the SSU gene evolves fast enough to accumulate substitutions between
186 Glomeromycotina speciation events (Bruns et al., 2018) and (ii) evaluate the biological
187 relevance of the VT and various EUs delineations. For each clade, we reconstructed
188 Bayesian phylogenetic trees of haplotypes (Supplementary Methods 1). We then ran
189 GMYC analyses (splits R-package (Ezard, Fujisawa, & Barraclough, 2009)) on each of these
190 trees and evaluated the support of the GMYC model compared to a null model in which
191 all tips are assumed to be different species, using a likelihood ratio test (LRT). If the LRT
192 supports the GMYC model, different SSU haplotypes belong to the same
193 Glomeromycotina species, *i.e.* the SSU rRNA gene has time to accumulate substitutions
194 between Glomeromycotina speciation events.

195

196 **Total diversity estimates:**

197

198 We evaluated how thoroughly sampled our species-level Glomeromycotina
199 phylogenetic trees are by estimating the total number of VT and EUs using rarefaction
200 curves and the Bayesian Diversity Estimation Software (BDES (Quince, Curtis, & Sloan,
201 2008)) (Supplementary Methods 3). The BDES estimates the total number of species by
202 extrapolating a sampled taxa abundance distribution at global scale (Quince et al., 2008).

203

204 **Additional molecular markers:**

205

206 We explored the possibility to carry some of our analyses using two other molecular
207 markers: the large subunit (LSU) rRNA gene and the ITS2 region. We downloaded the
208 Glomeromycotina LSU database of Delavaux et al. (2020) as well as the LSU sequences
209 available in MaarjAM. We obtained a total 2,044 sequences that we aligned using MAFFT
210 and TrimAl. We retained the 1,760 unique haplotypes, reconstructed the phylogenetic tree
211 of the LSU sequences using BEAST2 and used the resulting calibrated tree to delineate
212 Glomeromycotina LSU units with the GMYC model (same pipeline as above). We similarly
213 downloaded the Glomeromycotina ITS dataset of Lekberg et al. (2018). We tried to align
214 them but confirmed that the ITS sequences of Glomeromycotina are very difficult to align,
215 making them unsuitable for phylogenetic reconstruction and subsequent diversification
216 analyses (Supplementary Fig. 1).

217

218 **Diversification analyses:**

219

220 Unless specified differently, our diversification analyses were performed using the
221 SSU rRNA gene. In order to account for various sources of uncertainties in the SSU rRNA
222 data, we replicated all our diversification analyses across different species delineations,
223 phylogenetic reconstructions and dating, and total diversity estimates. For each species
224 delineation criterion, we obtained a consensus tree and selected 12 trees equally spaced in

225 4 independent Bayesian chains, hereafter referred to as the replicate trees. When the 12
226 trees were not sufficient to conclude, we used 100 replicate trees.

227

228 We estimated lineage-specific speciation rates using ClaDS, a Bayesian
229 diversification model that accounts for speciation rate heterogeneity by modeling small
230 rate shifts at speciation events (Maliot, Hartig, & Morlon, 2019). At each speciation event,
231 the descending lineages inherit new speciation rates sampled from a log-normal
232 distribution with an expected value $\log[\alpha \times \lambda]$ (where λ represents the parental speciation
233 rate and α is a trend parameter) and a standard deviation σ . We considered the model with
234 constant turnover ε (*i.e.* constant ratio between extinction and speciation rates; *ClaDS2*) and
235 ran a newly-developed ClaDS algorithm based on data augmentation techniques which
236 enables us to estimate mean rates through time (Maliot & Morlon, 2022). We ran ClaDS
237 with 3 independent chains, checked their convergence using a Gelman-Rubin diagnostic
238 criterion (Gelman & Rubin, 1992), and recorded lineage-specific speciation rates. We also
239 recorded the estimated hyperparameters (α , σ , ε) and the value $m = \alpha \times \exp(\sigma^2/2)$, which
240 indicates the general trend of the rate through time (Maliot et al., 2019). We replicated these
241 analyses using the LSU gene.

242

243 In addition, we applied CoMET (TESS R-package (Höhna, May, & Moore, 2016;
244 May, Höhna, & Moore, 2016)), another diversification approach that does not consider rate
245 variation across lineages, but models temporal shifts in speciation and extinction rates
246 affecting all lineages simultaneously. CoMET is a piecewise-constant model in a Bayesian
247 framework. We chose the Bayesian priors according to maximum likelihood estimates
248 from TreePar (Stadler, 2011), disallowed or not mass extinction events, and ran the MCMC
249 chains until convergence (minimum effective sample sizes of 500).

250

251 We also fitted a series of time-dependent and environment-dependent birth-death
252 diversification models using RPANDA (Condamine, Rolland, & Morlon, 2013; Morlon et
253 al., 2016) to confirm the observed temporal trends and test the influence of temperature,

254 pCO₂, and land plant fossil diversity on rates of Glomeromycotina speciation. For the time-
255 dependent models, we considered models with constant or exponential variation of
256 speciation rates through time and null or constant extinction rates (*fit_bd* function). As
257 extinction is notoriously hard to estimate from reconstructed phylogenies (Rabosky, 2016),
258 we tested the robustness of the inferred temporal trend in speciation when fixing
259 arbitrarily high levels of extinction (Supplementary Methods 4). For the environment-
260 dependent models, we considered an exponential dependency of the speciation rates with
261 the environmental variable (*env*), *i.e.* speciation rate= $b \cdot \exp(a \cdot \text{env})$, where *a* and *b* are two
262 parameters estimated by maximum likelihood (*fit_env* function). Best-fit models were
263 selected based on the corrected Akaike information criterion (AICc), considering that a
264 difference of 2 in AICc indicates that the model with the lowest AICc is better. We
265 replicated these analyses using the LSU gene.

266

267 The influence of temperature was tested on the complete Glomeromycotina
268 phylogenetic trees, using estimates of past global temperature (Royer, Berner, Montañez,
269 Tabor, & Beerling, 2004). We also carried a series of simulation analyses to test the
270 robustness of our temperature-dependent results (Supplementary Methods 5). The
271 influence of pCO₂ (Foster, Royer, & Lunt, 2017) and of land plant fossil diversity was tested
272 starting from 400 Myr ago, as these environmental data are not available for more ancient
273 times. For these analyses we sliced the phylogenies at 400 and 200 Myr ago, and applied
274 the diversification models to the sliced sub-trees larger than 50 tips. Estimates of land plant
275 diversity were obtained using all available Embryophyta fossils from the Paleobiology
276 database (<https://paleobiodb.org>) and using the shareholder quorum subsampling method
277 (Supplementary Methods 6; (Alroy, 2010)).

278

279 We considered missing species in all our diversification analyses by imputing
280 sampling fractions, computed as the number of observed VT or EUs divided by the
281 corresponding BDES estimates of global Glomeromycotina diversity (Table 1). We used a
282 global sampling fraction for all Glomeromycotina, as the main Glomeromycotina clades

283 had a similar sampling fraction (Supplementary Table 2). To assess the robustness of our
284 results to global diversity estimates, we replicated all diversification analyses using a range
285 of lower sampling fractions (from 90% to 50%, *i.e.* assuming that only that percentage of
286 the global Glomeromycotina species diversity is in fact represented in our dataset).

287
288 **Testing for correlates of present-day Glomeromycotina speciation rates:**

289
290 To further investigate the potential factors correlating with Glomeromycotina
291 speciation rates, we assessed the relationship between lineage-specific estimates of
292 present-day speciation rates (obtained with the ClADS analyses) and characteristics of each
293 Glomeromycotina taxonomic unit, *i.e.* VT or EUs.

294
295 First, to assess the effect of specialization on speciation rates, we characterized
296 Glomeromycotina relative niche width using a set of 10 abiotic and biotic variables
297 recorded in MaarjAM database for each Glomeromycotina unit. In short, among a curated
298 dataset containing Glomeromycotina sequences occurring only in natural ecosystems
299 (dataset 2; Supplementary Table 2; Perez-Lamarque et al., 2020), for each Glomeromycotina
300 unit, we reported the number of continents, ecosystems, climatic zones, biogeographic
301 realms, habitats, and biomes where it was sampled, as well as its number of plant partners,
302 their phylogenetic diversity, and its centrality in the plant-fungus bipartite network, and
303 performed a principal component analysis (PCA; Supplementary Methods 7). For
304 Glomeromycotina units represented by at least 10 sequences, we tested whether these PCA
305 coordinates reflecting Glomeromycotina niche widths were correlated with the present-
306 day speciation rates using both linear mixed-models (not accounting for phylogeny) or
307 MCMCglmm models (Hadfield, 2010). For MCMCglmm, we assumed a Gaussian residual
308 distribution, included the fungal phylogenetic tree as a random effect, and ran the MCMC
309 chains for 1,300,000 iterations with a burn-in of 300,000 and a thinning interval of 500.

310

311 Next, we tested the relationship between speciation rates and geographic
312 characteristics of Glomeromycotina units. To evaluate the effect of latitude on speciation
313 rates, we associated each Glomeromycotina unit with its set of latitudes and used similar
314 MCMCglmm with an additional random effect corresponding to the Glomeromycotina
315 unit. To account for inhomogeneous sampling along the latitudinal gradient, we re-ran the
316 model on jackknifed datasets (we re-sampled 1,000 interactions per slice of latitude of
317 twenty degrees). Similarly, we tested the effect of climatic zone and habitat on speciation
318 rates.

319
320 Then, to assess the effect of dispersal capacity on speciation rates, we evaluated the
321 relationship between spore size and speciation rate for the few ($n=32$) VT that contain
322 sequences of morphologically characterized Glomeromycotina isolates (Davison et al.,
323 2018). We gathered measures of their average spore length (Davison et al., 2018) and tested
324 their relationship with speciation rate by using a phylogenetic generalized least square
325 regression (PGLS).

326
327 Finally, as a first attempt at connecting Glomeromycotina macroevolutionary
328 diversification to microevolutionary processes, we measured intraspecific genetic
329 diversities across Glomeromycotina units. For each Glomeromycotina unit containing at
330 least 10 sequences, we computed genetic diversity using Tajima's estimator (Tajima,
331 1983)($\theta\pi$; Supplementary Methods 8). Using similar statistical tests as above, we
332 investigated the correlation of Glomeromycotina genetic diversity with speciation rate,
333 niche width, geographic characteristics, and spore size. We tested the robustness of the
334 results to the minimal number of sequences per Glomeromycotina unit (10, 15, or 20) used
335 to compute genetic diversity and to perform the PCA.

336
337 These statistical models were replicated on the different phylogenetic trees
338 (consensus or replicates) for each delineation and we reported p-values (P) corresponding
339 to two-sided tests.

340

341 **Simulation analyses:**

342

343 The use of a short and slowly evolving gene such as the central region of the SSU
344 rRNA gene to delineate species may lead to an artificial lumping of species into the same
345 unit that would reduce the number of phylogenetic branching events toward the present
346 and result in a biased inference of temporal diversification dynamics, including an
347 artifactual detection of a diversification slowdown (Moen & Morlon, 2014). We used
348 simulations mimicking the evolution of the SSU rRNA gene as *Glomeromycotina*
349 diversified to quantify this potential bias.

350

351 We simulated the diversification of a clade of species in the last 505 Myr, according
352 to two scenarios: (i) constant speciation rate and no extinction and (ii) constant speciation
353 and extinction rates (Supplementary Figure 2a). To model intraspecific differentiation, we
354 added intraspecific splits on these simulated species trees by grafting coalescent events at
355 each tip: for each species, we uniformly sampled between 2 and 15 individuals and we
356 considered that all these individuals had to coalesce before the last speciation event; the
357 age of the coalescent tree within each species was uniformly sampled between 0 and the
358 age of the last speciation event (with a maximum of 30 Myr). We used the functions *pbtree*
359 and *rcoal* from the R-packages *phytools* and *ape* (Paradis, Claude, & Strimmer, 2004;
360 Revell, 2012) to simulate the species phylogenies and the intraspecific coalescences
361 respectively. We used two net diversification rates ($r=0.010$ and $r=0.015$) for simulating the
362 species phylogenies, in order to reach a total number of species similar to that obtained
363 with our empirical data when using the VT and EU99 delineations, respectively. Next, we
364 simulated the evolution of short 520 bp DNA sequences on the obtained trees, using the
365 function *simulate_alignment* (R-package HOME; Perez-Lamarque & Morlon, 2019). We
366 used a substitution rate of 0.001 event per Myr and only 25% of variable sites, which
367 resulted in an alignment that mimicked the *Glomeromycotina* SSU rDNA alignment. We
368 performed 10 simulations per scenario. For each of these simulations we kept the unique

369 haplotypes at present and applied the same pipelines as above, using the EU99 species
370 delineation criteria: after delineating the EU99 units, we reconstructed the EU99
371 phylogenetic trees, ran the ClaDS analyses on these trees, and recorded mean estimated
372 speciation rates at present and 50, 100, and 150 Myr ago.

373 **Results:**

374

375 **Glomeromycotina species delineations & phylogenetic reconstructions:**

376

377 We automatically delineated Glomeromycotina into evolutionary units (EU) using
378 a monophyly criterion and several thresholds of SSU rRNA sequence similarity (from 97%
379 to 99%). The EU97.5 and EU98 delineations (obtained using a threshold of 97.5% and 98%
380 respectively) provided a number of Glomeromycotina units (340 and 641) relatively
381 comparable to the 384 currently recognized *virtual taxa* (VT), while the EU97 delineation
382 had much less units (182). Conversely, the EU98.5 and EU99 delineations yielded a much
383 larger number of Glomeromycotina units (1,190 and 2,647). These numbers obtained with
384 the EU98.5 and EU99 delineations were consistent with the numbers obtained using GMYC
385 analyses, which delineate species-like units based on detecting when splitting events in the
386 haplotype tree start to follow branching patterns consistent with intra-specific
387 differentiations (*i.e.* coalescent patterns) instead of speciation events (*i.e.* birth-death
388 patterns; Supplementary Tables 3, 4, & 5). The GMYC results therefore support the idea
389 that some VT might lump together several cryptic species (Bruns et al.,
390 2018)(Supplementary Note 1), and that a 98.5 or 99% similarity threshold is more relevant
391 for Glomeromycotina species delineation. In addition, the GMYC model is significantly
392 supported over the model where all SSU rRNA haplotypes correspond to a different
393 species (GMYC LRT: $P < 0.05$; Supplementary Fig. 3), with on average 10 SSU haplotypes
394 per species-like unit, and a mean intraspecific sequence similarity of 99% (Supplementary
395 Table 5 & Supplementary Fig. 3). This indicates that the region of the SSU marker used to
396 characterized Glomeromycotina evolves fast enough to accumulate substitutions between
397 Glomeromycotina speciation events, meaning that it is an informative (although not
398 perfect) marker for delineating Glomeromycotina species-like units. In comparison, the
399 same pipeline carried on the LSU database delineated only 181 GMYC units, suggesting
400 that it was much less complete than the SSU database. We replicated the subsequent

401 diversification analyses using the LSU region, even though we put more trust in our results
402 using the SSU database given the incompleteness of the LSU database.

403

404 Rarefaction curves as well as BDES (Bayesian Diversity Estimation Software) and
405 Chao2 estimates of diversity suggested that more than 90% of the total Glomeromycotina
406 diversity is represented in our SSU dataset regardless of the delineation threshold (Fig. 1,
407 Table 1, Supplementary Tables 5 & 6), which is consistent with the proportion of new
408 Glomeromycotina units detected in recent studies (Sepp et al., 2019).

409

410 The reconstructed Bayesian phylogenetic trees based on VT and EU delineations did
411 not yield high support for the nodes separating the main Glomeromycotina orders; yet, the
412 trees had no significantly-supported conflicts either, and similar branching times of the
413 internal nodes overall (Fig. 2, Supplementary Fig. 4). As expected, finer delineations
414 resulted in an increase in the number of nodes close to the present (Supplementary Fig. 5).
415 However, we observed a slowdown in the accumulation of new lineages close to the
416 present in all lineage through time plots (LTTs), including those with the finest delineations
417 (EU98.5 and EU99; Supplementary Fig. 6).

418

419 **Temporal diversification dynamics:**

420

421 We found that speciation rates for Glomeromycotina ranged from 0.005 to 0.03
422 events per lineage per Myr, using both the VT and EU SSU rRNA delineations (Fig. 2;
423 Supplementary Fig. 7). Speciation rates varied both within and among Glomeromycotina
424 orders, with Glomerales and Diversisporales having the highest present-day speciation
425 rates (Supplementary Fig. 8). As expected we observed higher present-day speciation rates
426 for finer delineations, but at the haplotype level (i.e. at the level of the individual SSU rRNA
427 sequences within each unit) we found a significant correlation of present-day speciation
428 rates computed with ClADS using different delineations (Supplementary Fig. 9). Whatever
429 the delineations, Glomeromycotina experienced their highest speciation rates between 200

430 and 100 Myr ago according to estimates obtained with ClaDS (Fig. 2; Supplementary Fig.
431 10) and between 150 and 50 Myr ago according to CoMET (Fig. 2; Supplementary Fig. 11).
432 ClaDS estimates of speciation rates at 150 Myr ago were 26% (\pm s.d. 17) higher than those
433 at 300 Myr with the EU99 delineation. With the VT delineation, the increase was of 3% (\pm 8).
434 The peak was even stronger using CoMET: 30% \pm 20 higher at 150 Myr in comparison to
435 300 Myr with the EU99 delineation (71% \pm 40 with the VT delineation; Fig. 2).

436

437 The peak of speciation rates was followed by a decline in the recent past (Fig. 2;
438 Supplementary Fig. 10), as suggested by the plateauing of the LTTs. A global decline of the
439 speciation rates through time was independently supported by ClaDS and CoMET
440 analyses, as well as time-dependent models in RPANDA (Morlon, Parsons, & Plotkin,
441 2011)(Supplementary Figs. 11, 12, & 13). This speciation rate decline was robust to all
442 species delineations, the branching process prior (Supplementary Table 7), phylogenetic
443 uncertainty, and assumed sampling fractions as low as 50%, except in ClaDS analyses
444 where the trend disappeared in some EU99 trees and for sampling fractions lower than
445 70% (Supplementary Figs. 14 & 15). We also found a period of high speciation rates
446 between 200 and 100 Myr ago followed by a decline in our analyses with the LSU region,
447 for assumed sampling fractions as low as 60% (Supplementary Figure 16).

448

449 We did not find a strong signal of extinction in our analyses: the turnover rate
450 estimated from ClaDS was generally close to zero (Supplementary Fig. 12b), and models
451 including extinctions were never selected in RPANDA (Supplementary Fig. 13). Similarly,
452 the extinction rates estimated in piecewise-constant models (CoMET) were not
453 significantly different from 0 and we did not find significant support for mass extinction
454 events (Supplementary Fig. 17). Yet, forcing the extinction rate to high positive values did
455 not modify the general trend of speciation rate slowdown (Supplementary Figs. 18 & 19).

456

457

458 **Correlates of Glomeromycotina diversification:**

459

460 When fitting environment-dependent models of diversification, we found that
461 temperature-dependent models better fit Glomeromycotina diversification than time-
462 dependent models, with higher speciation rates during warm climatic periods (Fig. 3;
463 Supplementary Fig. 20). This was true for all Glomeromycotina delineations, sampling
464 fractions, and crown ages (Supplementary Figs. 21, 22, 23, & 24), with the exception of some
465 EU99 trees with a 50% sampling fraction (Supplementary Fig. 24). It was also true in our
466 analyses using the LSU region, for sampling fractions down to 50% (Supplementary Figure
467 29). This signal of temperature dependency was not due to a temporal trend
468 (Supplementary Figs. 25 & 26) nor to an artefact caused by rate heterogeneities
469 (Supplementary Fig. 27). Evidence for temperature dependency, however, decreased in
470 some clades closer to the present, as small trees tend to be best fit by constant or time-
471 depend models (Supplementary Fig. 28). We detected a significant positive dependency of
472 the speciation rates on CO₂ concentrations in some sub-trees, but rarely found a significant
473 effect of plant fossil diversity (Supplementary Fig. 28).

474

475 The PCA of Glomeromycotina relative niche width characteristics had a first
476 principal component (PC1) that indicated the propensity of each Glomeromycotina unit
477 (VT or EUs) to be vastly distributed among continents, ecosystems and/or associated with
478 many plant species and lineages (*i.e.* high generalism), whereas the second principal
479 component (PC2) indicated the propensity of a given Glomeromycotina unit to associate
480 with few plant species on many continents (*i.e.* high specialism toward plants;
481 Supplementary Figs. 30, 31, & 32). Hence, PC1 reflects Glomeromycotina niche width,
482 whereas PC2 discriminates the width of the abiotic relatively to the biotic niche (Fig. 4a-b).
483 We found a positive correlation between lineage-specific speciation rates and PC1 in the
484 majority of the VT and EU99 trees, but no significant correlation with PC2 (Fig. 4c-d;
485 Supplementary Fig. 33a). However, these results were no longer significant when
486 controlling for phylogenetic non-independence between Glomeromycotina units
487 (Supplementary Fig. 33b), likely because a single *Glomeraceae* clade, including the abundant

488 and widespread morphospecies *Rhizophagus irregularis* and *R. clarus* (high PC1 values), had
489 both the highest speciation rates and the largest niche widths among Glomeromycotina
490 (Supplementary Fig. 34).

491
492 Although Glomeromycotina diversity is currently higher in the (sub)tropics
493 (Supplementary Fig. 35), we found no effect of latitude on speciation rates, regardless of
494 the Glomeromycotina delineation or the minimum number of sequences per
495 Glomeromycotina unit (MCMCglmm: $P > 0.05$). In addition, we actually did not detect a
496 higher total number of Glomeromycotina species in grasslands compared to forests
497 (Supplementary Figure 36; confirming the results of Davison et al. 2015), and it is thus not
498 surprising that we reported no effect of habitat or climatic zone on speciation rates
499 (Supplementary Fig. 37), suggesting that tropical grasslands are not particular
500 diversification hotspots for Glomeromycotina. Similarly, we recovered no significant
501 correlation between spore size and speciation rate (Supplementary Fig. 38), nor between
502 spore size and level of endemism (Supplementary Fig. 39).

503
504 Finally, Tajima's estimator of Glomeromycotina genetic diversity was significantly
505 and positively correlated with niche width (PC1) for all Glomeromycotina delineations and
506 minimal number of sequences per Glomeromycotina unit considered, and in particular
507 with abiotic aspects of the niche (PC2) in many cases (Fig. 4e-h; Supplementary Fig. 33).
508 Genetic diversity was not correlated with speciation rate (Supplementary Fig. 33), latitude,
509 habitat, climatic zone (MCMCglmm: $P > 0.05$), or spore size (PGLS: $P > 0.05$).

510 511 **Simulation results:**

512
513 When we simulated the evolution of a short DNA gene mimicking the SSU rRNA
514 marker and used it to delineate species, we found that the number of EU99 delineated units
515 was generally lower than the number of simulated species (~10% to 20% lower;
516 Supplementary Figure 2b). Hence, even the EU99 delineation tends to lump together some

517 closely related species. As expected, this lumping resulted in an artefactual inference of a
518 decline of speciation rates toward the present, but this artifactual decline was significantly
519 smaller in magnitude than that observed in Glomeromycotina (Figure 5). Hence, these
520 analyses suggest that the lumping of species resulting from the use of a small, slowly
521 evolving marker is unlikely to fully explain the strong temporal decline in speciation rate
522 we found in Glomeromycotina.

523 **Discussion**

524

525 **Glomeromycotina species delineations, diversity, and phylogeny:**

526

527 It is difficult to delineate species in Glomeromycotina, which are poorly
528 differentiated morphologically and mainly characterized by environmental sequences
529 (Bruns et al., 2018). Our GMYC analyses suggest that Glomeromycotina species-like units
530 correspond to SSU rRNA haplotypes with a sequence similarity between 98.5 and 99%.
531 With this criterion of species delineation, we estimate that there are between 1,300 and
532 2,900 Glomeromycotina ‘species’. These estimates are largely above the number of
533 currently described morphospecies or VT (Supplementary Note 1) but remain low in
534 comparison with other fungal groups, like the Agaricomycetes that include taxa forming
535 ectomycorrhiza (Varga et al., 2019).

536

537 Our phylogenies based on the SSU rRNA gene did not resolve the branching of the
538 Glomeromycotina orders, with node supports similar to those of previous studies (Davison
539 et al., 2015; Krüger et al., 2012; Rimington et al., 2018)(Supplementary Note 2). These
540 findings confirm that additional genomic evidence is required to reach consensus. We
541 considered this uncertainty in species delineation and phylogenetic reconstruction by
542 repeating our diversification analyses across species delineation criteria and on a set of
543 trees spanning the likely tree space. We found effects of species delineation consistent with
544 *a priori* expectations: criteria that lump together more dissimilar sequences (e.g. those that
545 use a lower percentage of similarity cut-off) result in lower diversity estimates, lower
546 estimates of speciation rates, and patterns of diversification through time that reflect longer
547 terminal branch-lengths, such as peaks of diversification that occur earlier. Despite this
548 variability, we found that general patterns, such as the observed temporal decline in
549 speciation rates and the significant association between temperature and speciation rates,
550 were consistent across species delineations and trees. Therefore, our study based on a short
551 SSU (or LSU) rRNA region should encourage both efforts to obtain more genetic data,

552 including longer reads (Krehenwinkel et al., 2019; Tedersoo, Albertsen, Anslan, &
553 Callahan, 2021) and additional genomic information, with the aim of reconstructing better
554 supported, comprehensive phylogenies and efforts to conduct diversification analyses
555 despite uncertainty in the data for groups where better data is not yet available.

556

557 **Glomeromycotina diversify slowly:**

558

559 We found speciation rates for Glomeromycotina an order of magnitude lower than
560 rates typically found for macro-eukaryotes (Maliet et al., 2019; Upham et al., 2019), like
561 plants (Zanne et al., 2014), or Agaricomycetes (Varga et al., 2019). Low speciation rates in
562 Glomeromycotina may be linked to their multinucleate hyphal state (Yildirim, Malar,
563 Kokkoris, & Corradi, 2020), to their occasional long-distance dispersal that homogenizes
564 populations globally over evolutionary timescales (Savary et al., 2018), and/or to the fact
565 that they are generalist obligate symbionts (Morlon, Kemp, Plotkin, & Brisson, 2012).
566 Regardless of the proximal cause, and contrary to Agaricomycetes for example, which
567 present a large diversity of species, morphologies, and ecologies, Glomeromycotina have
568 poorly diversified in the last 500 Myr despite their ubiquity; their niche space is restricted
569 to plant roots and the surrounding soil because of their obligate dependence on plants for
570 more than 400 Myr (Rich, Nouri, Courty, & Reinhardt, 2017; Tisserant et al., 2013).

571

572 Our estimates of speciation rates were highly variable across lineages. We reported
573 the highest speciation rates in Glomeraceae and Diversisporaceae. Speciation rates in
574 Paraglomeraceae and Archaeosporaceae, which are thought to be less beneficial for the
575 plants than the fast diversifying Glomeraceae and Diversisporaceae (Säle et al., 2021), were
576 an order of magnitude lower. We can therefore speculate that good symbiotic abilities may
577 favor diversification, although this remains to be tested in further investigations.

578

579 We found little evidence for species extinction in Glomeromycotina, including at
580 mass extinction events. Because Glomeromycotina are relatively widespread and have a

581 an ancient tendency toward generalism, they might therefore be quite resilient to land
582 plant mass extinctions and low extinction rates have been predicted before based on their
583 ecology (Morton, 1990). Yet, these low extinction rate estimates could also come from the
584 difficulty of estimating extinction from molecular phylogenies (Rabosky, 2016), one of the
585 limitations of phylogeny-based diversification analyses (Supplementary Note 3). Fossils of
586 Glomeromycotina that can be ascribed to species or genera are too scarce to support or
587 conflict with this finding.

588

589 **Glomeromycotina diversification through time:**

590

591 The observed peak of Glomeromycotina speciations detected between 200 and 100
592 Myr (or 150-50 Myr depending on the models) was mainly linked to the frequent
593 speciations in the largest family Glomeraceae. This peak was concomitant with the
594 radiation of flowering plants (Sauquet & Magallón, 2018), but also with a major continental
595 reconfiguration, including the breakdown of Pangea and the formation of climatically
596 contrasted landmasses (Davison et al., 2015). This period was also characterized by a warm
597 climate potentially directly or indirectly favorable to Glomeromycotina diversification,
598 such that disentangling the impact of these various factors on Glomeromycotina
599 diversification rates is not straightforward. Interestingly, a peak of speciations at this
600 period was also found in the Agaricomycetes, a clade of fungi including lineages forming
601 ectomycorrhizae (Varga et al., 2019).

602

603 This peak in the occurrence of speciation events was followed by a decline in
604 speciation rates. The detection of temporal declines in speciation rates in phylogenetic
605 diversification analyses can sometimes be artifactual, for example if some species are
606 incorrectly lumped together during species delineation or if the proportion of species not
607 represented in the phylogeny is under-estimated (Moen & Morlon, 2014). We considered
608 these potential biases, conducted sensitivity analyses, and found that the observed
609 slowdown was robust, and even amplified under scenarios of high extinction. Some

610 Glomeromycotina species are likely lumped together into the same SSU haplotypes
611 (Krüger et al., 2012), but both our use of an overly small assumed sampling intensity (50%)
612 and our simulation analyses demonstrated that this lumping is not sufficient to explain the
613 observed slowdown. In addition, we also detected a temporal decline in speciation rates
614 when using another marker (the LSU rRNA gene).

615
616 Temporal declines in speciation rates have been observed in many clades, including
617 microorganisms (Condamine, Rolland, & Morlon, 2019; Morlon et al., 2012; Rabosky &
618 Lovette, 2008). They have often been interpreted as a progressive reduction of the number
619 of available niches as species diversify and accumulate (Moen & Morlon, 2014; Rabosky,
620 2009). In Glomeromycotina, this potential effect of niche saturation could be exacerbated
621 by a reduction of their niches linked to both repetitive breakdowns of their symbiosis with
622 plants and climatic changes. Indeed, since the Cretaceous, many plant lineages evolved
623 alternative root symbioses or became non-symbiotic (Brundrett & Tedersoo, 2018;
624 Maherali, Oberle, Stevens, Cornwell, & McGlenn, 2016; Selosse & Le Tacon, 1998; Werner
625 et al., 2018): approximately 20% of extant plants do not interact with Glomeromycotina
626 anymore (van der Heijden et al., 2015). Additionally, the cooling of the Earth during the
627 Cenozoic reduced the surface of tropical regions (Meseguer & Condamine, 2020; Ziegler et
628 al., 2003), which tend to be a reservoir of ecological niches for Glomeromycotina (Brundrett
629 & Tedersoo, 2018; Davison et al., 2015; Read, 1991).

630
631 The difficulty of reconstructing past symbiotic associations prevents direct testing
632 the hypothesis that the emergence of new root symbioses in plants led to a decline in
633 speciation rates in Glomeromycotina. However, we tested the hypothesis that global
634 temperature changes affected speciation rates and found a strong relationship. Such
635 associations between temperature and speciation rates have been observed before in
636 eukaryotes and have several potential causes (Condamine et al., 2019). In particular, the
637 productivity hypothesis states that resources and associated ecological niches are more
638 numerous in warm and productive environments, especially when the tropics are large,

639 which entail higher speciation rates (Clarke & Gaston, 2006). This hypothesis is particularly
640 relevant for Glomeromycotina, which have many host plant niches in the tropics, as shown
641 by their latitudinal diversity gradient, and potentially relatively less in temperate and polar
642 regions (Toussaint et al., 2020), where a higher proportion of plants are non-mycorrhizal
643 (Bueno et al., 2017) or ectomycorrhizal (Brundrett & Tedersoo, 2018; Varga et al., 2019).
644 Hence, the observed effect of past global temperatures could reflect the shrinkage of
645 tropical areas and the associated decrease of the relative proportion of arbuscular
646 mycorrhizal plants. Future developments of diversification models incorporating
647 interspecific interactions would allow us to better test these hypotheses.

648
649 A few Glomeromycotina clades displayed a significant support for diversification
650 models with a positive dependency of speciation rates on CO₂ concentrations, which
651 reinforces the idea that for the corresponding Glomeromycotina, benefits retrieved from
652 plants could have been amplified by high CO₂ concentrations and fostered diversification
653 (Field et al., 2016; Humphreys et al., 2010). Conversely, we found a limited effect of land
654 plant fossil diversity, which indicates that variations in the tempo of Glomeromycotina
655 diversification did not systematically follow those of land plants. Still, the possible
656 concordance of the peak of Glomeromycotina speciations with the radiation of the
657 Angiosperms is noteworthy, in particular in Glomeraceae that frequently interact with
658 present-day Angiosperms (Rimington et al., 2018). Plant diversification might have
659 fostered the diversification of Glomeromycotina from the emergence of land plants until
660 the Mesozoic (Lutzoni et al., 2018; Morton, 1990), but less so thereafter, when
661 Glomeromycotina diversification declined while some flowering plants radiated,
662 including Glomeromycotina-associated groups, like the Poaceae, but also
663 Glomeromycotina-free groups such as the extraordinary radiation of Orchidaceae (Givnish
664 et al., 2015), blurring co-diversification patterns (Supplementary Fig. 40)(Cleal & Cascales-
665 Miñana, 2014; Ramírez-Barahona, Sauquet, & Magallón, 2020).

666

667 **Correlates of Glomeromycotina recent speciation rates:**

668

669 Looking at the correlates of Glomeromycotina present-day speciation rates, we found
670 no effect of habitat or climatic zone, even though Glomeromycotina are more frequent and
671 diverse in the tropics (Davison et al., 2015; Pärtel et al., 2017; Toussaint et al., 2020) and a
672 positive correlation with global temperature. Further work, including a more thorough
673 sampling of the distribution of Glomeromycotina species across latitudes and habitats,
674 would be required to confirm these patterns and to distinguish whether speciation events
675 are indeed no more frequent in the tropics or, if they are, whether long-distance dispersal
676 redistributes the new lineages at different latitudes over long time scales. Contrary to
677 previous predictions (Pärtel et al., 2017), we did not find that tropical grasslands are
678 diversification hotspots for Glomeromycotina; we actually did not even find higher
679 Glomeromycotina species richness in (tropical) grasslands *versus* forests at global scale, in
680 agreement with Davison *et al.* (2015).

681

682 Similarly, although the temporal changes in the availability of Glomeromycotina
683 niches likely influenced the diversification of the group, we found little support for
684 Glomeromycotina species with larger niche width having higher lineage-specific
685 speciation rates. We also note that there are important aspects of the niche that we do not
686 (and yet cannot) account for in our characterization of Glomeromycotina niche width: it is
687 thought that some Glomeromycotina species may mainly provide mineral nutrients
688 extracted from the soil, whereas others may be more specialized in protecting plants from
689 biotic or abiotic stresses (Chagnon, Bradley, Maherali, & Klironomos, 2013) and such (inter-
690 or intra-specific) functional variations may have evolutionary significance. Finally,
691 although spore size is often inversely related to dispersal capacity (Nathan et al., 2008),
692 which can limit speciation by increasing gene flow, we found no significant correlation
693 between spore size and speciation rates, which may be explained either by a weak or absent
694 effect or by the low number of species for which this data is available. In addition, the
695 absence of correlation between spore size and level of endemism suggests that even
696 Glomeromycotina with large spores experience long-distance dispersal (Davison et al.,

697 2018; Kivlin, 2020). Thus, if large spores might limit dispersal at smaller (*e.g.* intra-
698 continental) scales in Glomeromycotina (Bueno & Moora, 2019; Chaudhary, Nolim, Sosa-
699 Hernández, Egan, & Kastens, 2020), this does not seem to affect speciation rates.

700

701 In Glomeromycotina, intraspecific variability is an important source of functional
702 diversity (Munkvold, Kjølner, Vestberg, Rosendahl, & Jakobsen, 2004; Savary et al., 2018)
703 and their genetic diversity may indicate the intraspecific variability on which selection can
704 act, potentially leading to speciation. Here, geographically widespread Glomeromycotina
705 species appear to be more genetically diverse, as previously suggested by population
706 genomics (Savary et al., 2018), but do not necessarily speciate more frequently. Along with
707 a decoupling between genetic diversity and lineage-specific speciation rate, this suggests
708 that the accumulation of genetic diversity in the SSU region among distant subpopulations
709 is not enough to spur Glomeromycotina speciation.

710

711 **Analyzing diversification dynamics using a short marker gene:**

712

713 Short DNA regions, like those used in metabarcoding surveys, typically do not
714 allow to robustly delineate species, estimate global-scale diversity, and reconstruct
715 phylogenetic trees. As these three aspects can all affect results of diversification analyses
716 (Moen & Morlon, 2014), such analyses are rarely performed with these types of data. Yet,
717 for many species-rich groups of organisms, in particular microorganisms, no other data
718 currently provide a thorough representation of diversity at the “species” level. Hence,
719 these data, although far from ideal, are the only one that can be used to study the past
720 diversification of such groups (see Lewitus et al., 2018; Louca et al., 2018 for antecedents).
721 The approach we took here is to recognize all these potential sources of uncertainty and
722 biases and to test the robustness of our results. We demonstrated the usefulness of this
723 approach: while some results inevitably depend on the choices made for species
724 delineation, phylogenetic reconstruction, and the estimation of global scale diversity,
725 others are sufficiently strong to hold despite uncertainty in the data. Our results therefore

726 illustrate that using a short DNA marker (e.g. a metabarcode) combined with intensive
727 sensitivity analyses can be useful for studying the diversification dynamics of poorly-
728 known groups.

729

730 **Conclusion:**

731

732 Our findings that Glomeromycotina have low speciation rates, likely constrained by
733 the availability of suitable niches, reinforce the vision of Glomeromycotina as an
734 “evolutionary cul-de-sac” (Malloch, 1987). We interpret the significant decline in
735 speciation rates toward the present as the conjunction of the emergence of plant lineages
736 not associated with Glomeromycotina and the reduction of tropical areas induced by
737 climate cooling, in the context of obligate dependence of Glomeromycotina on plants.
738 Temporal declines in speciation rates have often been interpreted as the signal of adaptive
739 radiations (Harmon, Schulte, Larson, & Losos, 2003; Moen & Morlon, 2014), that is clades
740 that experienced a rapid accumulation of morphological, ecological, and species diversity
741 (Simpson, 1953). Conversely, Glomeromycotina provide here a striking example of a clade
742 with slow morphological, ecological, and species diversification that features a pattern of
743 temporal decline in speciation rates, that might reflect the reduction of the global
744 availability of their mycorrhizal niches.

745

746

747 **Acknowledgment:**

748

749 The authors acknowledge C. Strullu-Derrien, M. Elias, D. de Vienne, A. Vogler, J.-Y.
750 Dubuisson, C. Quince, S.-K. Sepp, and M. Chase for helpful discussions. They also thank
751 L. Aristide, S. Lambert, J. Clavel, I. Quintero, I. Overcast, and G. Sommeria for comments
752 on the manuscript, D. Marsh for English editing, and the Editor and three reviewers for
753 improvements of an earlier version of this manuscript. BPL acknowledges B. Robira, F.
754 Foutel-Rodier, F. Duchenne, E. Faure, E. Kerdoncuff, R. Petrolli, and G. Collobert for useful

755 discussions and C. Fruciano and E. Lewitus for providing codes. This work was supported
756 by a doctoral fellowship from the École Normale Supérieure de Paris attributed to BPL and
757 the École Doctorale FIRE – Programme Bettencourt. MÖ was supported by the European
758 Regional Development Fund (Centre of Excellence EcolChange) and University of Tartu
759 (PLTOM20903). Funding of the research of FM was from the Agence Nationale de la
760 Recherche (ANR-19-CE02-0002). HM acknowledges support from the European Research
761 Council (grant CoG-PANDA).

762 **References:**

- 763 Alroy, J. (2010). Geographical, environmental and intrinsic biotic controls on Phanerozoic
764 marine diversification. *Palaeontology*, 53(6), 1211–1235. doi:10.1111/j.1475-
765 4983.2010.01011.x
- 766 Barnosky, A. D. (2001). Distinguishing the effects of the red queen and court jester on
767 miocene mammal evolution in the northern rocky mountains. *Journal of Vertebrate*
768 *Paleontology*, 21(1), 172–185. doi:10.1671/0272-4634(2001)021[0172:DTEOTR]2.0.CO;2
- 769 Benton, M. J. (2009). The Red Queen and the Court Jester: Species diversity and the role of
770 biotic and abiotic factors through time. *Science*, 323(5915), 728–732.
771 doi:10.1126/science.1157719
- 772 Bouckaert, R., Heled, J., Kühnert, D., Vaughan, T., Wu, C.-H., Xie, D., ... Drummond, A. J.
773 (2014). BEAST 2: A software platform for Bayesian evolutionary analysis. *PLoS*
774 *Computational Biology*, 10(4), e1003537. doi:10.1371/journal.pcbi.1003537
- 775 Bredenkamp, G. J., Spada, F., & Kazmierczak, E. (2002). On the origin of northern and
776 southern hemisphere grasslands. *Plant Ecology*, 163(2), 209–229.
777 doi:10.1023/A:1020957807971
- 778 Brundrett, M. C., & Tedersoo, L. (2018). Evolutionary history of mycorrhizal symbioses
779 and global host plant diversity. *New Phytologist*, 220(4), 1108–1115.
780 doi:10.1111/nph.14976
- 781 Bruns, T. D., Corradi, N., Redecker, D., Taylor, J. W., & Öpik, M. (2018).
782 Glomeromycotina: what is a species and why should we care? *New Phytologist*,
783 220(4), 963–967. doi:10.1111/nph.14913
- 784 Bueno, C. G., & Moora, M. (2019). How do arbuscular mycorrhizal fungi travel? *New*
785 *Phytologist*, 222(2), 645–647. doi:10.1111/nph.15722
- 786 Bueno, C. G., Moora, M., Gerz, M., Davison, J., Öpik, M., Pärtel, M., ... Zobel, M. (2017).
787 Plant mycorrhizal status, but not type, shifts with latitude and elevation in Europe.
788 *Global Ecology and Biogeography*, 26(6), 690–699. doi:10.1111/geb.12582
- 789 Chagnon, P.-L., Bradley, R. L., Maherali, H., & Klironomos, J. N. (2013). A trait-based
790 framework to understand life history of mycorrhizal fungi. *Trends in Plant Science*,

791 18(9), 484–491. doi:10.1016/j.tplants.2013.05.001

792 Chaudhary, V. B., Nolimal, S., Sosa-Hernández, M. A., Egan, C., & Kastens, J. (2020).
793 Trait-based aerial dispersal of arbuscular mycorrhizal fungi. *New Phytologist*, 228(1),
794 238–252. doi:10.1111/nph.16667

795 Chomicki, G., Kiers, E. T., & Renner, S. S. (2020). The evolution of mutualistic
796 dependence. *Annual Review of Ecology, Evolution, and Systematics*, 51(1), 409–432.
797 doi:10.1146/annurev-ecolsys-110218-024629

798 Clarke, A., & Gaston, K. J. (2006). Climate, energy and diversity. *Proceedings of the Royal*
799 *Society B: Biological Sciences*, 273(1599), 2257–2266. doi:10.1098/rspb.2006.3545

800 Cleal, C. J., & Cascales-Miñana, B. (2014). Composition and dynamics of the great
801 Phanerozoic Evolutionary Floras. *Lethaia*, 47(4), 469–484. doi:10.1111/let.12070

802 Condamine, F. L., Rolland, J., Höhna, S., Sperling, F. A. H., & Sanmartín, I. (2018). Testing
803 the role of the Red Queen and Court Jester as drivers of the macroevolution of
804 Apollo butterflies. *Systematic Biology*, 67(6), 940–964. doi:10.1093/sysbio/syy009

805 Condamine, F. L., Rolland, J., & Morlon, H. (2013). Macroevolutionary perspectives to
806 environmental change. *Ecology Letters*, 16(SUPPL.1), 72–85. doi:10.1111/ele.12062

807 Condamine, F. L., Rolland, J., & Morlon, H. (2019). Assessing the causes of diversification
808 slowdowns: temperature-dependent and diversity-dependent models receive
809 equivalent support. *Ecology Letters*, 22(11), 1900–1912. doi:10.1111/ele.13382

810 Correia, M., Heleno, R., da Silva, L. P., Costa, J. M., & Rodríguez-Echeverría, S. (2019).
811 First evidence for the joint dispersal of mycorrhizal fungi and plant diaspores by
812 birds. *New Phytologist*, 222(2), 1054–1060. doi:10.1111/nph.15571

813 Davison, J., Moora, M., Öpik, M., Adholeya, A., Ainsaar, L., Bâ, A., ... Zobel, M. (2015).
814 Global assessment of arbuscular mycorrhizal fungus diversity reveals very low
815 endemism. *Science*, 349(6251), 970–973. doi:10.1126/science.aab1161

816 Davison, J., Moora, M., Öpik, M., Ainsaar, L., Ducousso, M., Hiiesalu, I., ... Zobel, M.
817 (2018). Microbial island biogeography: isolation shapes the life history characteristics
818 but not diversity of root-symbiotic fungal communities. *The ISME Journal*, 12(9),
819 2211–2224. doi:10.1038/s41396-018-0196-8

820 Delavaux, C. S., Sturmer, S. L., Wagner, M. R., Schütte, U., Morton, J. B., & Bever, J. D.
821 (2020). Utility of large subunit for environmental sequencing of arbuscular
822 mycorrhizal fungi: a new reference database and pipeline. *New Phytologist*, 1–5.
823 doi:10.1111/nph.17080

824 Egan, C., Li, D.-W., & Klironomos, J. (2014). Detection of arbuscular mycorrhizal fungal
825 spores in the air across different biomes and ecoregions. *Fungal Ecology*, 12, 26–31.
826 doi:10.1016/j.funeco.2014.06.004

827 Ezard, T., Fujisawa, T., & Barraclough, T. G. (2009). SPLITS: SPecies' Limits by Threshold
828 Statistics. R-package.

829 Feijen, F. A., Vos, R. A., Nuytinck, J., & Merckx, V. S. F. T. (2018). Evolutionary dynamics
830 of mycorrhizal symbiosis in land plant diversification. *Scientific Reports*, 8(1), 10698.
831 doi:10.1038/s41598-018-28920-x

832 Field, K. J., Pressel, S., Duckett, J. G., Rimington, W. R., & Bidartondo, M. I. (2015).
833 Symbiotic options for the conquest of land. *Trends in Ecology & Evolution*, 30(8), 477–
834 486. doi:10.1016/j.tree.2015.05.007

835 Field, K. J., Rimington, W. R., Bidartondo, M. I., Allinson, K. E., Beerling, D. J., Cameron,
836 D. D., ... Pressel, S. (2016). Functional analysis of liverworts in dual symbiosis with
837 Glomeromycota and Mucoromycotina fungi under a simulated Palaeozoic CO₂
838 decline. *ISME Journal*, 10(6), 1514–1526. doi:10.1038/ismej.2015.204

839 Foster, G. L., Royer, D. L., & Lunt, D. J. (2017). Future climate forcing potentially without
840 precedent in the last 420 million years. *Nature Communications*, 8(1), 14845.
841 doi:10.1038/ncomms14845

842 Fujisawa, T., & Barraclough, T. G. (2013). Delimiting species using single-locus data and
843 the generalized mixed yule coalescent approach: A revised method and evaluation
844 on simulated data sets. *Systematic Biology*, 62(5), 707–724. doi:10.1093/sysbio/syt033

845 Gelman, A., & Rubin, D. B. (1992). Inference from iterative simulation using multiple
846 sequences. *Statistical Science*, 7(4), 457–472. doi:10.1214/ss/1177011136

847 Givnish, T. J., Spalink, D., Ames, M., Lyon, S. P., Hunter, S. J., Zuluaga, A., ... Cameron,
848 K. M. (2015). Orchid phylogenomics and multiple drivers of their extraordinary

849 diversification. *Proceedings of the Royal Society B: Biological Sciences*, 282(1814),
850 20151553. doi:10.1098/rspb.2015.1553

851 Hadfield, J. D. (2010). MCMC methods for multi-response generalized linear mixed
852 models: The MCMCglmm R package. *Journal of Statistical Software*, 33(2), 1–22.
853 doi:10.18637/jss.v033.i02

854 Harmon, L. J., Schulte, J. A., Larson, A., & Losos, J. B. (2003). Tempo and mode of
855 evolutionary radiation in iguanian lizards. *Science*, 301(5635), 961–964.
856 doi:10.1126/science.1084786

857 Höhna, S., May, M. R., & Moore, B. R. (2016). TESS: An R package for efficiently
858 simulating phylogenetic trees and performing Bayesian inference of lineage
859 diversification rates. *Bioinformatics*, 32(5), 789–791. doi:10.1093/bioinformatics/btv651

860 Humphreys, C. P., Franks, P. J., Rees, M., Bidartondo, M. I., Leake, J. R., & Beerling, D. J.
861 (2010). Mutualistic mycorrhiza-like symbiosis in the most ancient group of land
862 plants. *Nature Communications*, 1(8), 103. doi:10.1038/ncomms1105

863 James, T. Y., Kauff, F., Schoch, C. L., Matheny, P. B., Hofstetter, V., Cox, C. J., ... Vilgalys,
864 R. (2006). Reconstructing the early evolution of Fungi using a six-gene phylogeny.
865 *Nature*, 443(7113), 818–822. doi:10.1038/nature05110

866 Janzen, T., & Etienne, R. S. (2017). Inferring the role of habitat dynamics in driving
867 diversification: evidence for a species pump in Lake Tanganyika cichlids. *BioRxiv*,
868 11(2), 1–18. doi:https://doi.org/10.1101/085431

869 Katoh, K., & Standley, D. M. (2013). MAFFT Multiple sequence alignment software
870 version 7: Improvements in performance and usability. *Molecular Biology and*
871 *Evolution*, 30(4), 772–780. doi:10.1093/molbev/mst010

872 Kivlin, S. N. (2020). Global mycorrhizal fungal range sizes vary within and among
873 mycorrhizal guilds but are not correlated with dispersal traits. *Journal of*
874 *Biogeography*, 47(9), 1994–2001. doi:10.1111/jbi.13866

875 Krehenwinkel, H., Pomerantz, A., Henderson, J. B., Kennedy, S. R., Lim, J. Y., Swamy, V.,
876 ... Prost, S. (2019). Nanopore sequencing of long ribosomal DNA amplicons enables
877 portable and simple biodiversity assessments with high phylogenetic resolution

878 across broad taxonomic scale. *GigaScience*, 8(5). doi:10.1093/gigascience/giz006

879 Krüger, M., Krüger, C., Walker, C., Stockinger, H., & Schüßler, A. (2012). Phylogenetic
880 reference data for systematics and phylotaxonomy of arbuscular mycorrhizal fungi
881 from phylum to species level. *New Phytologist*, 193(4), 970–984. doi:10.1111/j.1469-
882 8137.2011.03962.x

883 Lee, J., Lee, S., & Young, J. P. W. (2008). Improved PCR primers for the detection and
884 identification of arbuscular mycorrhizal fungi. *FEMS Microbiology Ecology*, 65(2), 339–
885 349. doi:10.1111/j.1574-6941.2008.00531.x

886 Lekberg, Y., Vasar, M., Bullington, L. S., Sepp, S.-K. K., Antunes, P. M., Bunn, R., ... Öpik,
887 M. (2018). More bang for the buck? Can arbuscular mycorrhizal fungal communities
888 be characterized adequately alongside other fungi using general fungal primers?
889 *New Phytologist*, 220(4), 971–976. doi:10.1111/nph.15035

890 Lewitus, E., Bittner, L., Malviya, S., Bowler, C., & Morlon, H. (2018). Clade-specific
891 diversification dynamics of marine diatoms since the Jurassic. *Nature Ecology and*
892 *Evolution*, 2(11), 1715–1723. doi:10.1038/s41559-018-0691-3

893 Louca, S., Shih, P. M., Pennell, M. W., Fischer, W. W., Parfrey, L. W., & Doebeli, M. (2018).
894 Bacterial diversification through geological time. *Nature Ecology and Evolution*, 2(9),
895 1458–1467. doi:10.1038/s41559-018-0625-0

896 Lutzoni, F., Nowak, M. D., Alfaro, M. E., Reeb, V., Miadlikowska, J., Krug, M., ...
897 Magallón, S. (2018). Contemporaneous radiations of fungi and plants linked to
898 symbiosis. *Nature Communications*, 9(1), 1–11. doi:10.1038/s41467-018-07849-9

899 Magallón, S., & Sanderson, M. J. (2001). Absolute diversification rates in angiosperm
900 clades. *Evolution*, 55(9), 1762–1780. doi:10.1111/j.0014-3820.2001.tb00826.x

901 Maherali, H., Oberle, B., Stevens, P. F., Cornwell, W. K., & McGlenn, D. J. (2016).
902 Mutualism persistence and abandonment during the evolution of the mycorrhizal
903 symbiosis. *American Naturalist*, 188(5), E113–E125. doi:10.1086/688675

904 Maliet, O., Hartig, F., & Morlon, H. (2019). A model with many small shifts for estimating
905 species-specific diversification rates. *Nature Ecology & Evolution*, 3(7), 1086–1092.
906 doi:10.1038/s41559-019-0908-0

907 Maliet, O., & Morlon, H. (2022). Fast and accurate estimation of species-specific
908 diversification rates using data augmentation. *Systematic Biology*, 71(2), 353–366.
909 doi:10.1093/sysbio/syab055

910 Malloch, D. M. (1987). The evolution of mycorrhizae. *Can. J. Plant. Path.*, 9, 398–402.

911 May, M. R., Höhna, S., & Moore, B. R. (2016). A Bayesian approach for detecting the
912 impact of mass-extinction events on molecular phylogenies when rates of lineage
913 diversification may vary. *Methods in Ecology and Evolution*, 7(8), 947–959.
914 doi:10.1111/2041-210X.12563

915 Meseguer, A. S., & Condamine, F. L. (2020). Ancient tropical extinctions at high latitudes
916 contributed to the latitudinal diversity gradient. *Evolution*, 74(9), 1966–1987.
917 doi:10.1111/evo.13967

918 Moen, D., & Morlon, H. (2014). Why does diversification slow down? *Trends in Ecology
919 and Evolution*, 29(4), 190–197. doi:10.1016/j.tree.2014.01.010

920 Morlon, H. (2014). Phylogenetic approaches for studying diversification. *Ecology Letters*,
921 17(4), 508–525. doi:10.1111/ele.12251

922 Morlon, H., Kems, B. D., Plotkin, J. B., & Brisson, D. (2012). Explosive radiation of a
923 bacterial species group. *Evolution*, 66(8), 2577–2586. doi:10.1111/j.1558-
924 5646.2012.01598.x

925 Morlon, H., Lewitus, E., Condamine, F. L., Manceau, M., Clavel, J., & Drury, J. (2016).
926 RPANDA: An R package for macroevolutionary analyses on phylogenetic trees.
927 *Methods in Ecology and Evolution*, 7(5), 589–597. doi:10.1111/2041-210X.12526

928 Morlon, H., Parsons, T. L., & Plotkin, J. B. (2011). Reconciling molecular phylogenies with
929 the fossil record. *Proceedings of the National Academy of Sciences*, 108(39), 16327–16332.
930 doi:10.1073/pnas.1102543108

931 Morton, J. B. (1990). Species and clones of arbuscular mycorrhizal fungi (Glomales,
932 Zygomycetes): their role in macro- and microevolutionary processes. *Mycotaxon
933 (USA)*, 37, 493–515.

934 Munkvold, L., Kjølner, R., Vestberg, M., Rosendahl, S., & Jakobsen, I. (2004). High
935 functional diversity within species of arbuscular mycorrhizal fungi. *New Phytologist*,

936 164(2), 357–364. doi:10.1111/j.1469-8137.2004.01169.x

937 Nathan, R., Schurr, F. M., Spiegel, O., Steinitz, O., Trakhtenbrot, A., & Tsoar, A. (2008).
938 Mechanisms of long-distance seed dispersal. *Trends in Ecology & Evolution*, 23(11),
939 638–647. doi:10.1016/j.tree.2008.08.003

940 Öpik, M., Davison, J., Moora, M., & Zobel, M. (2014). DNA-based detection and
941 identification of Glomeromycota: the virtual taxonomy of environmental sequences.
942 *Botany*, 92(2), 135–147. doi:10.1139/cjb-2013-0110

943 Öpik, M., Vanatoa, A., Vanatoa, E., Moora, M., Davison, J., Kalwij, J. M., ... Zobel, M.
944 (2010). The online database MaarjAM reveals global and ecosystemic distribution
945 patterns in arbuscular mycorrhizal fungi (Glomeromycota). *New Phytologist*, 188(1),
946 223–241. doi:10.1111/j.1469-8137.2010.03334.x

947 Paradis, E., Claude, J., & Strimmer, K. (2004). APE: Analyses of phylogenetics and
948 evolution in R language. *Bioinformatics*, 20(2), 289–290.
949 doi:10.1093/bioinformatics/btg412

950 Pärtel, M., Öpik, M., Moora, M., Tedersoo, L., Szava-Kovats, R., Rosendahl, S., ... Zobel,
951 M. (2017). Historical biome distribution and recent human disturbance shape the
952 diversity of arbuscular mycorrhizal fungi. *New Phytologist*, 216(1), 227–238.
953 doi:10.1111/nph.14695

954 Perez-Lamarque, B., & Morlon, H. (2019). Characterizing symbiont inheritance during
955 host–microbiota evolution: Application to the great apes gut microbiota. *Molecular*
956 *Ecology Resources*, 19(6), 1659–1671. doi:10.1111/1755-0998.13063

957 Perez-Lamarque, B., Selosse, M. A., Öpik, M., Morlon, H., & Martos, F. (2020). Cheating
958 in arbuscular mycorrhizal mutualism: a network and phylogenetic analysis of
959 mycoheterotrophy. *New Phytologist*, 226(6), 1822–1835. doi:10.1111/nph.16474

960 Pons, J., Barraclough, T. G., Gomez-Zurita, J., Cardoso, A., Duran, D. P., Hazell, S., ...
961 Vogler, A. P. (2006). Sequence-based species delimitation for the DNA taxonomy of
962 undescribed insects. *Systematic Biology*, 55(4), 595–609.
963 doi:10.1080/10635150600852011

964 Powell, J. R., Monaghan, M. T., Öpik, M., & Rillig, M. C. (2011). Evolutionary criteria

965 outperform operational approaches in producing ecologically relevant fungal species
966 inventories. *Molecular Ecology*, 20(3), 655–666. doi:10.1111/j.1365-294X.2010.04964.x

967 Quince, C., Curtis, T. P., & Sloan, W. T. (2008). The rational exploration of microbial
968 diversity. *ISME Journal*, 2(10), 997–1006. doi:10.1038/ismej.2008.69

969 R Core Team. (2020). R: A language and environment for statistical computing. Vienna,
970 Austria: R Foundation for Statistical Computing.

971 Rabosky, D. L. (2009). Ecological limits and diversification rate: Alternative paradigms to
972 explain the variation in species richness among clades and regions. *Ecology Letters*,
973 12(8), 735–743. doi:10.1111/j.1461-0248.2009.01333.x

974 Rabosky, D. L. (2016). Challenges in the estimation of extinction from molecular
975 phylogenies: A response to Beaulieu and O'Meara. *Evolution*, 70(1), 218–228.
976 doi:10.1111/evo.12820

977 Rabosky, D. L., & Lovette, I. J. (2008). Density-dependent diversification in North
978 American wood warblers. *Proceedings of the Royal Society B: Biological Sciences*,
979 275(1649), 2363–2371. doi:10.1098/rspb.2008.0630

980 Ramírez-Barahona, S., Sauquet, H., & Magallón, S. (2020). The delayed and
981 geographically heterogeneous diversification of flowering plant families. *Nature*
982 *Ecology and Evolution*, 4(9), 1232–1238. doi:10.1038/s41559-020-1241-3

983 Read, D. J. (1991). Mycorrhizas in ecosystems. *Experientia*, 47(4), 376–391.
984 doi:10.1007/BF01972080

985 Revell, L. J. (2012). phytools: An R package for phylogenetic comparative biology (and
986 other things). *Methods in Ecology and Evolution*, 3(2), 217–223. doi:10.1111/j.2041-
987 210X.2011.00169.x

988 Rich, M. K., Nouri, E., Courty, P.-E., & Reinhardt, D. (2017). Diet of arbuscular
989 mycorrhizal fungi: Bread and butter? *Trends in Plant Science*, 22(8), 652–660.
990 doi:10.1016/j.tplants.2017.05.008

991 Rimington, W. R., Pressel, S., Duckett, J. G., Field, K. J., Read, D. J., & Bidartondo, M. I.
992 (2018). Ancient plants with ancient fungi: liverworts associate with early-diverging
993 arbuscular mycorrhizal fungi. *Proceedings of the Royal Society B: Biological Sciences*,

994 285(1888), 20181600. doi:10.1098/rspb.2018.1600

995 Rolland, J., Condamine, F. L., Jiguet, F., & Morlon, H. (2014). Faster speciation and
996 reduced extinction in the tropics contribute to the mammalian latitudinal diversity
997 gradient. *PLoS Biology*, 12(1), e1001775. doi:10.1371/journal.pbio.1001775

998 Royer, D. L., Berner, R. A., Montañez, I. P., Tabor, N. J., & Beerling, D. J. (2004). CO₂ as a
999 primary driver of Phanerozoic climate. *GSA Today*, 14(3), 4. doi:10.1130/1052-
1000 5173(2004)014<4:CAAPDO>2.0.CO;2

1001 Säle, V., Palenzuela, J., Azcón-Aguilar, C., Sánchez-Castro, I., da Silva, G. A., Seitz, B., ...
1002 Oehl, F. (2021). Ancient lineages of arbuscular mycorrhizal fungi provide little plant
1003 benefit. *Mycorrhiza*, 1–18. doi:10.1007/s00572-021-01042-5

1004 Sanders, I. R. (2003). Preference, specificity and cheating in the arbuscular mycorrhizal
1005 symbiosis. *Trends in Plant Science*, 8(4), 143–145. doi:10.1016/S1360-1385(03)00012-8

1006 Sauquet, H., & Magallón, S. (2018). Key questions and challenges in angiosperm
1007 macroevolution. *New Phytologist*, 219(4), 1170–1187. doi:10.1111/nph.15104

1008 Savary, R., Masclaux, F. G., Wyss, T., Droh, G., Cruz Corella, J., Machado, A. P., ...
1009 Sanders, I. R. (2018). A population genomics approach shows widespread
1010 geographical distribution of cryptic genomic forms of the symbiotic fungus
1011 *Rhizophagus irregularis*. *ISME Journal*, 12(1), 17–30. doi:10.1038/ismej.2017.153

1012 Selosse, M.-A., & Le Tacon, F. (1998). The land flora: a phototroph-fungus partnership?
1013 *Trends in Ecology & Evolution*, 13(1), 15–20. doi:10.1016/S0169-5347(97)01230-5

1014 Sepp, S. K., Davison, J., Jairus, T., Vasar, M., Moora, M., Zobel, M., & Öpik, M. (2019).
1015 Non-random association patterns in a plant–mycorrhizal fungal network reveal
1016 host–symbiont specificity. *Molecular Ecology*, 28(2), 365–378. doi:10.1111/mec.14924

1017 Simon, L., Bousquet, J., Lévesque, R. C., & Lalonde, M. (1993). Origin and diversification
1018 of endomycorrhizal fungi and coincidence with vascular land plants. *Nature*,
1019 363(6424), 67–69. doi:10.1038/363067a0

1020 Simon, L., Lalonde, M., & Bruns, T. D. (1992). Specific amplification of 18S fungal
1021 ribosomal genes from vesicular-arbuscular endomycorrhizal fungi colonizing roots.
1022 *Applied and Environmental Microbiology*, 58(1), 291–5.

- 1023 Simpson, G. G. (1953). *The major features of evolution*. New York: Columbia University
1024 Press.
- 1025 Smith, S. E., & Read, D. J. (2008). *Mycorrhizal Symbiosis*. *Mycorrhizal Symbiosis*. Elsevier.
1026 doi:10.1016/B978-0-12-370526-6.X5001-6
- 1027 Stadler, T. (2011). Mammalian phylogeny reveals recent diversification rate shifts.
1028 *Proceedings of the National Academy of Sciences*, 108(15), 6187–6192.
1029 doi:10.1073/pnas.1016876108
- 1030 Strullu-Derrien, C., Selosse, M.-A. A., Kenrick, P., & Martin, F. M. (2018). The origin and
1031 evolution of mycorrhizal symbioses: from palaeomycology to phylogenomics. *New*
1032 *Phytologist*, 220(4), 1012–1030. doi:10.1111/nph.15076
- 1033 Stürmer, S. L. (2012). A history of the taxonomy and systematics of arbuscular
1034 mycorrhizal fungi belonging to the phylum Glomeromycota. *Mycorrhiza*, 22(4), 247–
1035 258. doi:10.1007/s00572-012-0432-4
- 1036 Taberlet, P., Bonin, A., Zinger, L., & Coissac, E. (2018). DNA amplification and
1037 multiplexing. In *Environmental DNA* (Oxford Uni, pp. 41–57).
- 1038 Tajima, F. (1983). Evolutionary relationship of DNA sequences in finite populations.
1039 *Genetics*, 105(2), 437–460.
- 1040 Tedersoo, L., Albertsen, M., Anslan, S., & Callahan, B. (2021). Perspectives and benefits of
1041 high-throughput long-read sequencing in microbial ecology. *Applied and*
1042 *Environmental Microbiology*, 87(17), 1–19. doi:10.1128/AEM.00626-21
- 1043 Tisserant, E., Malbreil, M., Kuo, A., Kohler, A., Symeonidi, A., Balestrini, R., ... Martin, F.
1044 (2013). Genome of an arbuscular mycorrhizal fungus provides insight into the oldest
1045 plant symbiosis. *Proceedings of the National Academy of Sciences of the United States of*
1046 *America*, 110(50), 20117–20122. doi:10.1073/pnas.1313452110
- 1047 Toussaint, A., Bueno, G., Davison, J., Moora, M., Tedersoo, L., Zobel, M., ... Pärtel, M.
1048 (2020). Asymmetric patterns of global diversity among plants and mycorrhizal fungi.
1049 *Journal of Vegetation Science*, 31(2), 355–366. doi:10.1111/jvs.12837
- 1050 Upham, N. S., Esselstyn, J. A., & Jetz, W. (2019). Inferring the mammal tree: Species-level
1051 sets of phylogenies for questions in ecology, evolution, and conservation. *PLoS*

1052 *Biology*, 17(12), e3000494. doi:10.1371/journal.pbio.3000494

1053 van der Heijden, M. G. A. A., Martin, F. M., Selosse, M.-A. A., & Sanders, I. R. (2015).
1054 Mycorrhizal ecology and evolution: the past, the present, and the future. *New*
1055 *Phytologist*, 205(4), 1406–1423. doi:10.1111/nph.13288

1056 Varga, T., Krizsán, K., Földi, C., Dima, B., Sánchez-García, M., Sánchez-Ramírez, S., ...
1057 Nagy, L. G. (2019). Megaphylogeny resolves global patterns of mushroom evolution.
1058 *Nature Ecology & Evolution*, 3(4), 668–678. doi:10.1038/s41559-019-0834-1

1059 Venice, F., Ghignone, S., Salvioli di Fossalunga, A., Amselem, J., Novero, M., Xianan, X.,
1060 ... Bonfante, P. (2020). At the nexus of three kingdoms: the genome of the
1061 mycorrhizal fungus *Gigaspora margarita* provides insights into plant, endobacterial
1062 and fungal interactions. *Environmental Microbiology*, 22(1), 122–141. doi:10.1111/1462-
1063 2920.14827

1064 Werner, G. D. A., Cornelissen, J. H. C., Cornwell, W. K., Soudzilovskaia, N. A., Kattge, J.,
1065 West, S. A., & Kiers, E. T. (2018). Symbiont switching and alternative resource
1066 acquisition strategies drive mutualism breakdown. *Proceedings of the National*
1067 *Academy of Sciences*, 115(20), 5229–5234. doi:10.1073/pnas.1721629115

1068 Werner, G. D. A., Cornwell, W. K., Sprent, J. I., Kattge, J., & Kiers, E. T. (2014). A single
1069 evolutionary innovation drives the deep evolution of symbiotic N₂-fixation in
1070 angiosperms. *Nature Communications*, 5(1), 4087. doi:10.1038/ncomms5087

1071 Yildirim, G., Malar, M., Kokkoris, V., & Corradi, N. (2020). Parasexual and sexual
1072 reproduction in arbuscular mycorrhizal fungi: Room for both. *Trends in Microbiology*,
1073 28(7), 517–519. doi:10.1016/j.tim.2020.03.013

1074 Zanne, A. E., Tank, D. C., Cornwell, W. K., Eastman, J. M., Smith, S. A., FitzJohn, R. G., ...
1075 Beaulieu, J. M. (2014). Three keys to the radiation of angiosperms into freezing
1076 environments. *Nature*, 506(7486), 89–92. doi:10.1038/nature12872

1077 Ziegler, A. M., Eshel, G., McAllister Rees, P., Rothfus, T. A., Rowley, D. B., & Sunderlin,
1078 D. (2003). Tracing the tropics across land and sea: Permian to present. *Lethaia*, 36(3),
1079 227–254. doi:10.1080/00241160310004657

1080

1081 **Data Accessibility:**

1082

1083 All of the data used in this study are available in the open-access MaarjAM database
1084 (<https://maarjam.botany.ut.ee>). Spore lengths of Glomeromycotina were collected in the
1085 supplementary data of Davison et al. (2018). New scripts for delineating evolutionary units
1086 (EU) are available in the R-package RPANDA (through this GitHub branch for the
1087 moment: https://github.com/hmorlon/PANDA/tree/Benoit_phylosignal). The alignment of
1088 all the SSU rRNA sequences and their associated metadata publicly accessible through the
1089 Open Science Framework (osf) portal: osf.io/y2ts5.

1090

1091

1092 **Author contributions:**

1093

1094 All the authors designed the study. MÖ gathered the data and BPL performed the analyses.
1095 OM and ACAS provided some codes. BPL and HM wrote the first version of the
1096 manuscript and all authors contributed substantially to the revisions.

1097

1098 **Competing Interests statement:**

1099

1100 The authors declare that there is no conflict of interest.

1101

1102 **Tables:**

1103

1104 **Table 1: Estimation of the total diversity of Glomeromycotina:**

1105 Estimated sampling fraction using the Bayesian Diversity Estimation Software (BDES;
1106 Quince et al., 2008) for the different species delineations (VT or EU) assuming a Sichel
1107 species abundance distribution. The estimated number of units corresponds to the median
1108 value and we indicated the 95% confidence interval. We indicated the sampling fractions
1109 for each delineation, computed as the number of observed VT or EUs divided by the
1110 corresponding BDES estimates of global Glomeromycotina diversity.

1111 The Sichel distribution was selected compared to other distributions (log-normal, log-
1112 Student, and inverse gaussian) based on lowest deviance information criterion (DIC).

1113

Species delineation	Observed number of units	Estimated number of units	Sampling fraction	95% confidence interval	
				Lower boundary	Upper boundary
VT	384	403	95%	391 (98%)	422 (91%)
EU97	182	187	97%	183 (99%)	194 (94%)
EU97.5	340	357	95%	348 (98%)	370 (92%)
EU98	641	677	95%	663 (97%)	695 (92%)
EU98.5	1,190	1,268	94%	1,247 (95%)	1,293 (92%)
EU99	2,647	2,852	93%	2,817 (94%)	2,890 (92%)

1114

1115

1116 **Figures**

1117

1118

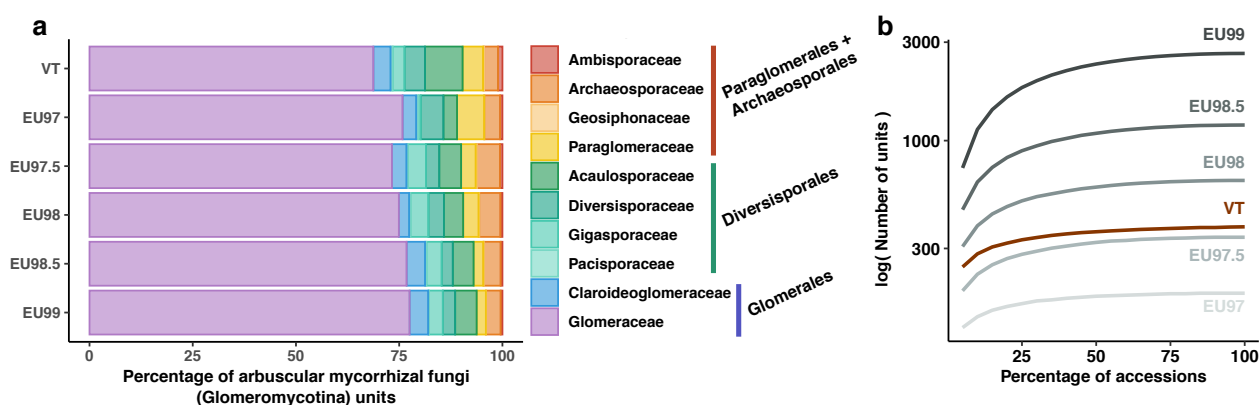
1119 **Figure 1: Molecular-based species delineations of Glomeromycotina (arbuscular**
1120 **mycorrhizal fungi) give consistent results and indicate a nearly complete sampling.**

1121 We compared the *virtual taxa* (VT) delineation from (Öpik et al., 2010) with newly-
1122 developed automatic delineations into *evolutionary units* (EUs) based on an average
1123 threshold of similarity and a criterion of monophyly.

1124 (a) The proportion of Glomeromycotina units (VT or EUs) in each Glomeromycotina family
1125 reveals constant proportions across delineations, although Glomeraceae tend to be
1126 relatively less abundant compared with the other Glomeromycotina family in the VT
1127 delineation. The main Glomeromycotina orders are indicated on the right of the charts:
1128 Paraglomerales + Archaeosporales, Diversisporales, and Glomerales (Glomeraceae +
1129 Claroideoglomeraceae).

1130 (b) Rarefaction curves indicating the number of Glomeromycotina units as a function of
1131 the percentage of sampled Glomeromycotina accession revealed that the
1132 Glomeromycotina sampling in MaarjAM is close to saturation for all delineations (VT or
1133 EUs). Rarefactions were performed 100 times every 5 percent and the median of the 100
1134 replicates is represented here.

1135



1136

1137 **Figure 2: The speciation dynamic of Glomeromycotina (arbuscular mycorrhizal fungi)**
1138 **varies significantly through time and between lineages.**

1139

1140 **(a-b):** Glomeromycotina consensus phylogenetic trees corresponding to the VT (a) and
1141 EU99 (b) species delineations. Branches are colored according to the lineage-specific
1142 speciation rates estimated by ClaDS using the BDES estimated sampling fraction: lineages
1143 with low and high speciation rates are represented in blue and red, respectively.

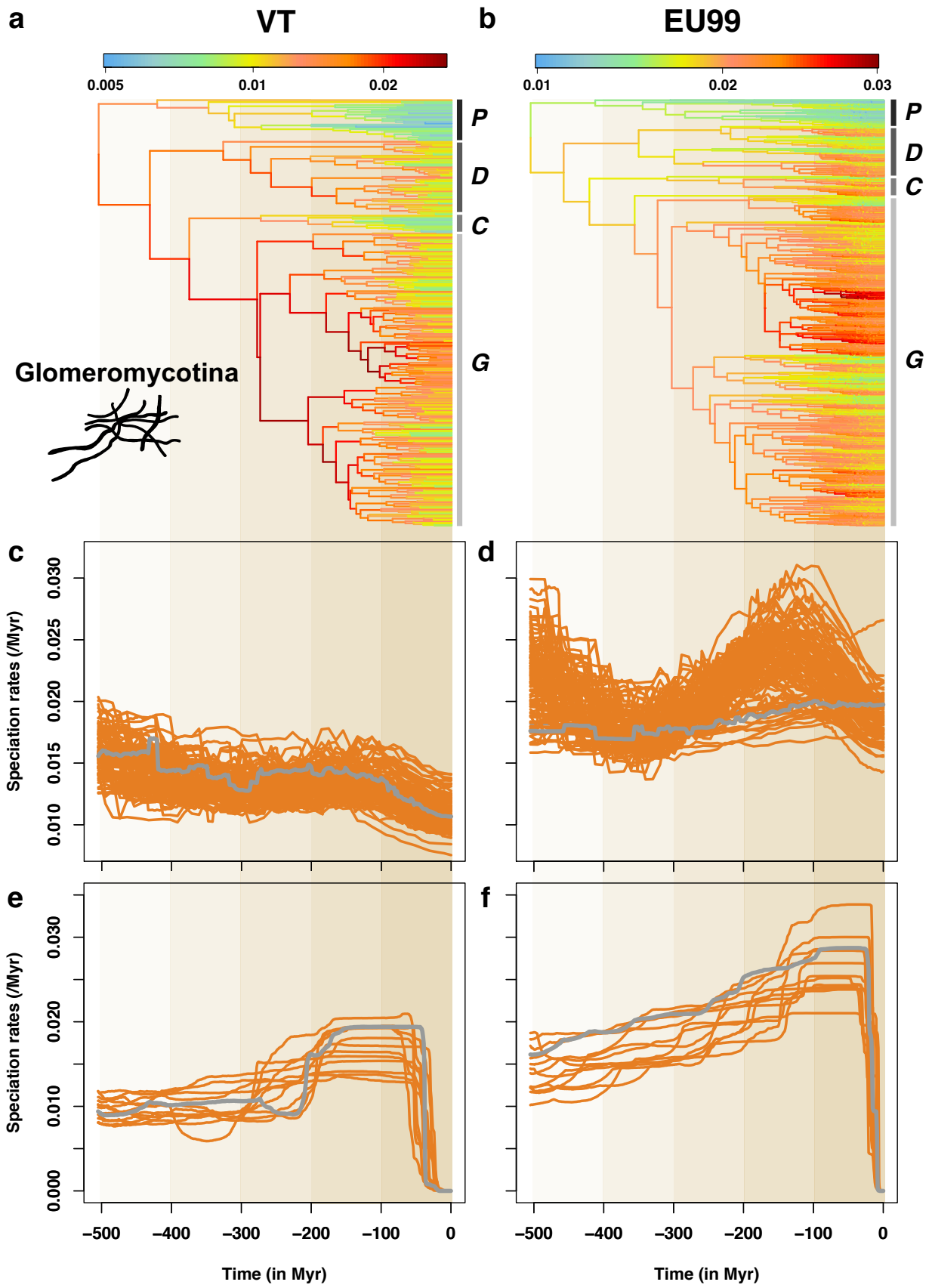
1144 The main Glomeromycotina clades are indicated with the following letters: *P* =
1145 Paraglomerales + Archaeosporales, *D* = Diversisporales, *C* = Claroideoglomeraceae, and *G*
1146 = Glomeraceae.

1147

1148 **(c-d):** Mean speciation rates through time estimated by ClaDS, for the VT (c) and EU99 (d)
1149 delineations and using the BDES estimated sampling fraction. The mean speciation rate
1150 corresponds to the maximum *a posteriori* (MAP) of the mean speciation rate across all
1151 fungal lineages back in time (including extinct and unsampled lineages). Orange and grey
1152 lines represent the independent replicate trees and the consensus tree, respectively:
1153 because some of the 12 replicate trees showed different trends, we replicated ClaDS
1154 inferences using 100 replicate trees. Unlike most replicate trees, the EU99 consensus tree
1155 tends to present a limited decline in speciation rates, which reinforces the idea that
1156 consensus trees can be misleading (Janzen & Etienne, 2017).

1157

1158 **(e-f):** Mean speciation rates through time estimated by CoMET, for the VT (c) and EU99 (d)
1159 delineations and using the BDES estimated sampling fraction. Orange and grey lines
1160 represent the 12 independent replicate trees and the consensus tree, respectively.



1162 **Figure 3: Temperature-dependent diversification models reveal that global temperature**
1163 **positively associates with the speciation rates of Glomeromycotina (arbuscular**
1164 **mycorrhizal fungi) in the last 500 million years.**

1165

1166 **(a):** Average global temperature in the last 500 million years (Myr) relative to the average
1167 temperature of the period 1960-1990. The smoothed orange line represents cubic splines
1168 with 33 degrees of freedom used to fit temperature-dependent models of
1169 Glomeromycotina diversification with RPANDA. This default smoothing was estimated
1170 using the R function *smooth.spline*.

1171

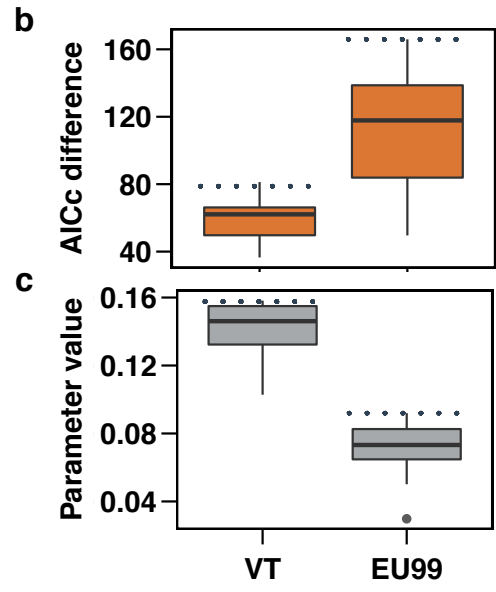
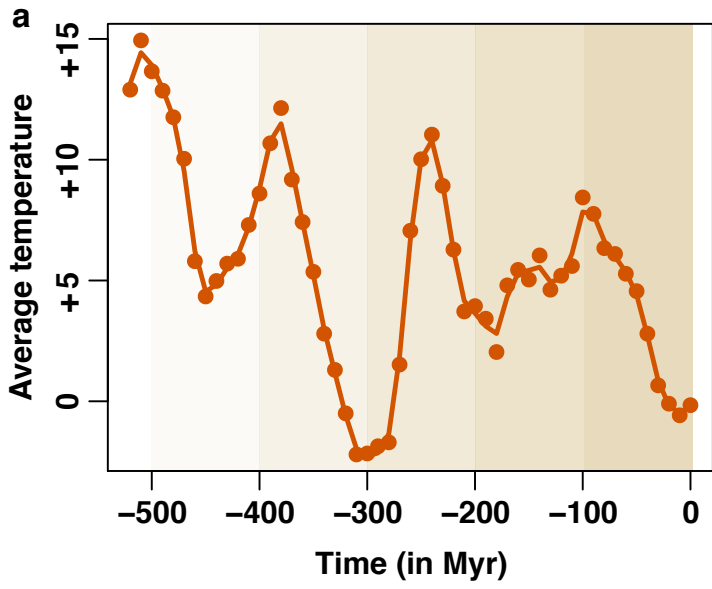
1172 **(b):** AICc difference between the best-supported time-dependent model and the
1173 temperature-dependent model in RPANDA, for the VT (left) and EU99 (right) delineations,
1174 using the BDES estimated sampling fraction. An AICc difference greater than 2 indicates
1175 that there is significant support for the temperature-dependent model.

1176

1177 **(c):** Parameter estimations of the temperature-dependent models (speciation rate \sim
1178 $\exp(\text{parameter} * \text{temperature})$). A positive parameter value indicates a positive effect of
1179 temperature on speciation rates.

1180

1181 For both delineations, the boxplots represent the results obtained for the consensus tree
1182 and the 12 independent replicate trees. Boxplots indicate the median surrounded by the
1183 first and third quartiles, and whiskers extend to the extreme values but no further than 1.5
1184 of the inter-quartile range. The horizontal dotted lines highlighted the values estimated for
1185 the consensus trees. Compared to the replicate trees, the consensus trees tends to present
1186 extreme values (stronger support for temperature-dependent model), which reinforces the
1187 idea that consensus trees can be a misleading representation (Janzen & Etienne, 2017).



1188

1189 **Figure 4: Abiotic and biotic correlates of speciation rates and genetic differentiation in**
1190 **Glomeromycotina (arbuscular mycorrhizal fungi)**

1191 **(a-b):** Projection of 10 abiotic and biotic variables on the two principal coordinates
1192 according to the VT (a) or EU99 (b) delineations. Principal coordinate analysis (PCA) was
1193 performed for the Glomeromycotina units represented by at least 10 sequences. Colors
1194 represent the contribution of the variable to the principal coordinates. The percentage for
1195 each principal coordinate (PC) indicates its amount of explained variance.

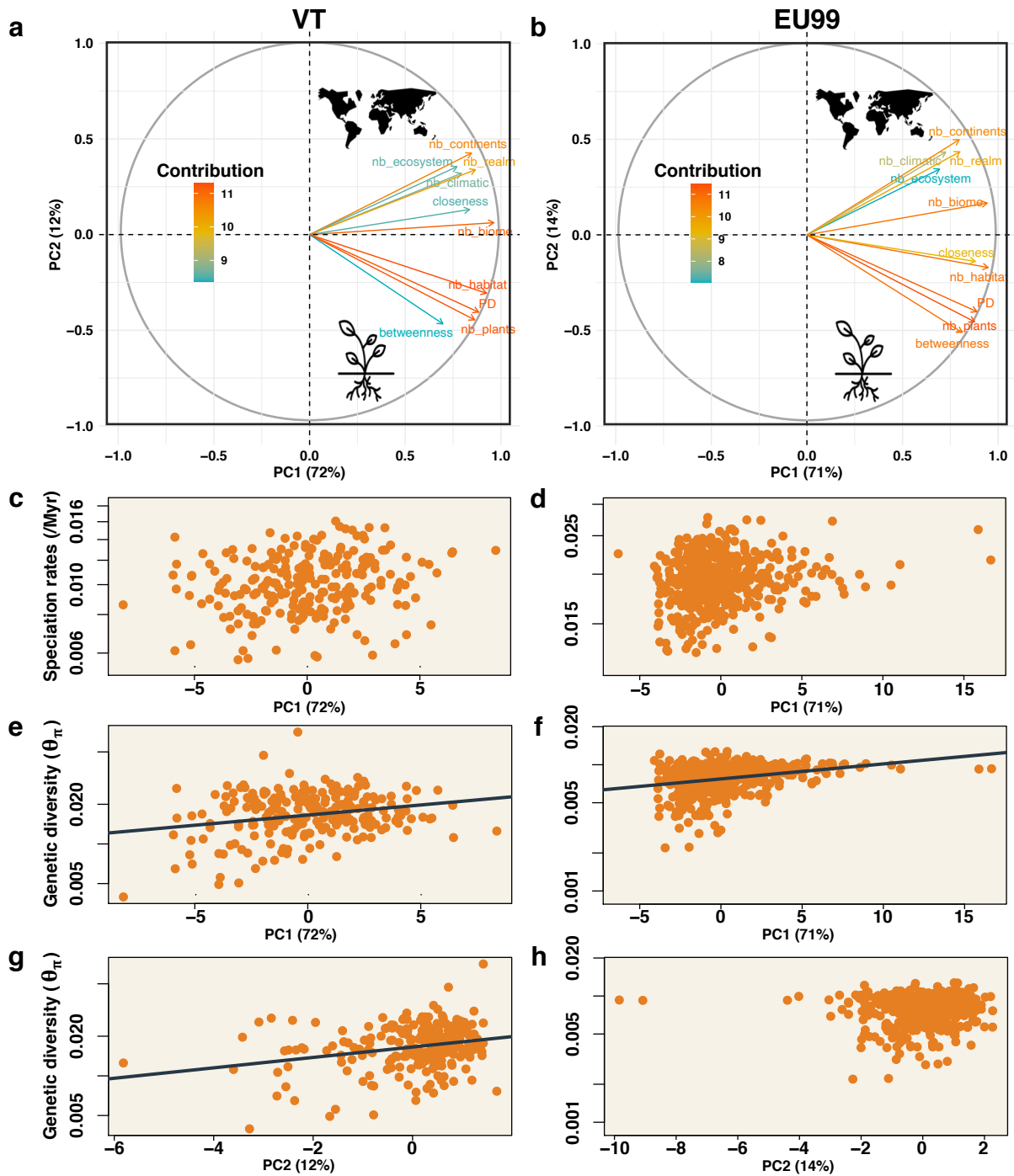
1196 Tested variables were: the numbers of continents on which the Glomeromycotina unit
1197 occurs (nb_continent), of realms (nb_realm), of ecosystems (nb_ecosystems), of habitats
1198 (nb_habitats), of biomes (nb_biomes), and climatic zones (nb_climatic) (Öpik et al., 2010),
1199 as well as information about the associated plant species of each unit, such as the number
1200 of plant partners (nb_plants), the phylogenetic diversity of these plants (PD), and the
1201 betweenness and closeness measurement of each fungal unit in the plant-fungus
1202 interaction network (see Methods).

1203

1204 **(c-d):** Speciation rates as a function of the PC1 coordinates for each VT (c) or EU99 (d) unit.
1205 Only the Glomeromycotina consensus tree is represented here (other replicate trees are
1206 presented in Supplementary Fig. 33).

1207

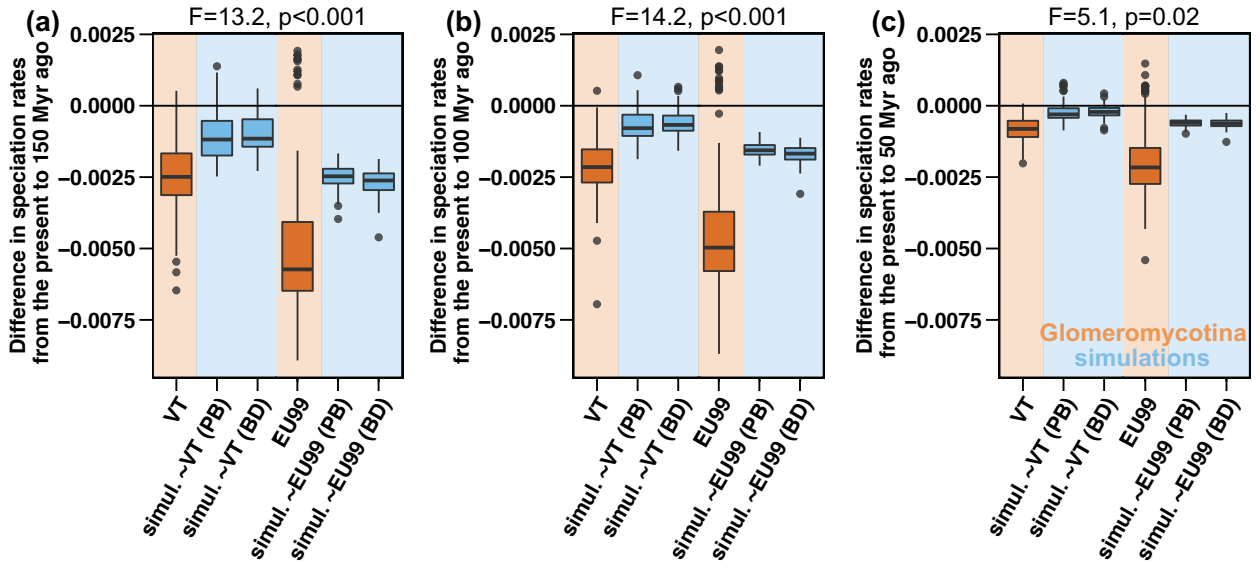
1208 **(e-h):** Genetic diversity (Tajima's $\theta\pi$ estimator) as a function of the PC1 (e-f) or PC2 (g-h)
1209 coordinates for each VT (e-g) or EU99 (f-h) unit. Only the Glomeromycotina consensus tree
1210 is represented here (other replicate trees are presented in Supplementary Fig. 33). The grey
1211 lines indicate the statistically significant linear regression between the two variables
1212 inferred using MCMCglmm.



1213

1214 **Figure 5: Artefactual species lumping and lack of phylogenetic resolution in the SSU**
1215 **rRNA region are not enough to explain the temporal decline in speciation rates detected**
1216 **in Glomeromycotina.**

1217 Comparison of the magnitude of the decline in speciation rates observed in
1218 Glomeromycotina (in orange) and on simulated data (in blue). The intensity of the
1219 slowdown is measured as the difference between the mean speciation rate estimated at
1220 present and the mean speciation rate estimated 150 Myr ago (a), 100 Myr ago (b), or 50 Myr
1221 ago (c). Negative differences indicate a speciation rate decline. Sequence alignments were
1222 simulated on phylogenetic trees obtained under a scenario of constant speciation rate and
1223 no extinction (*i.e.* pure birth "PB") and constant speciation and extinction rates (*i.e.* birth
1224 death "BD"), with characteristics mimicking the slow evolution of the SSU rRNA marker.
1225 We simulated phylogenies with two different net diversification rates, such that we
1226 obtained simulations with total numbers of species similar to the total numbers of VT or
1227 EU99 units (Supplementary Fig. 2). Boxplots indicate the median surrounded by the first
1228 and third quartiles, and whiskers extend to the extreme values but no further than 1.5 of
1229 the inter-quartile range. Each boxplot represents results for the consensus trees and the 12
1230 independent replicate trees for each of the 10 simulations, and for the consensus trees and
1231 the 100 independent replicate trees for the Glomeromycotina. Differences between the
1232 magnitude of the decline measured in Glomeromycotina (VT or EU99) and in the
1233 corresponding simulations were tested using linear models (reported at the top of the
1234 plots).



1235

1236 **Supplementary Tables Legends:**

1237

1238 **Supplementary Table 1:** Data selection in the MaarjAM database.

1239 **Supplementary Table 2:** Documented plant-Glomeromycotina interactions.

1240 **Supplementary Table 3:** Characteristics of the fungal units (VT or EU) in the database.

1241 **Supplementary Table 4:** Number of units (VT, EU, or GMYC) per fungal clades.

1242 **Supplementary Table 5:** GMYC delineation and corresponding sampling fraction.

1243 **Supplementary Table 6:** The estimated sampling fraction using Chao2 index suggested a
1244 sampling fraction >90%.

1245 **Supplementary Table 7:** The prior selection for the VT Bayesian phylogenetic
1246 reconstructions (BEAST) using nested sampling (NS) favored a log-normal and Pure-birth
1247 prior.

1248

1249 **Supplementary Figures Legends:**

1250

1251 **Supplementary Figure 1:** Visualization of Glomeromycotina sequence alignments: The
1252 ITS marker is not a good marker for Glomeromycotina phylogenetic reconstruction
1253 compared to the SSU rRNA region.

1254 **Supplementary Figure 2:** Simulated diversification scenarios.

1255 **Supplementary Figure 3:** GMYC species delineations in Glomeromycotina clades
1256 significantly support the existence of intraspecific haplotypes in the SSU rRNA gene.

1257 **Supplementary Figure 4:** Consensus Glomeromycotina phylogenetic trees for the different
1258 species delineations.

1259 **Supplementary Figure 5:** Node depth distribution of the consensus Glomeromycotina
1260 phylogenetic trees for the different delineations.

1261 **Supplementary Figure 6:** The accumulation of fungal lineages through time present a
1262 slowdown toward the present in the reconstructed Glomeromycotina phylogenetic trees.

1263 **Supplementary Figure 7:** Speciation rates per lineage estimated by ClaDS show that
1264 Glomeromycotina experienced heterogeneous diversification rates across clades and time.
1265 **Supplementary Figure 8:** Present-day speciation rates at the tips estimated by ClaDS show
1266 that Glomeromycotina have heterogeneous diversification rates across clades.
1267 **Supplementary Figure 9:** Speciation rates at the tips estimated by ClaDS for VT and EU
1268 delineations are significantly correlated.
1269 **Supplementary Figure 10:** The average speciation rates through time estimated by ClaDS
1270 show that Glomeromycotina experienced a decline in speciation rates toward the present
1271 after a period of high speciation rates.
1272 **Supplementary Figure 11:** The speciation rates through time estimated by CoMET show
1273 that Glomeromycotina experienced a decline in speciation rates toward the present after a
1274 period of high speciation rates.
1275 **Supplementary Figure 12:** Estimated hyperparameters of ClaDS2 runs, for the different
1276 Glomeromycotina delineations, using the BDES estimated sampling fraction.
1277 **Supplementary Figure 13:** The speciation rates through time estimated by RPANDA show
1278 that Glomeromycotina experienced a decline in speciation rates toward the present.
1279 **Supplementary Figure 14:** The speciation rates through time estimated by ClaDS also
1280 show that Glomeromycotina experienced a decline in speciation rates toward the present
1281 even when using sampling fractions <90%.
1282 **Supplementary Figure 15:** The speciation rates through time estimated by CoMET also
1283 show that Glomeromycotina experienced a decline in speciation rates toward the present
1284 even when using sampling fractions <90%.
1285 **Supplementary Figure 16:** Speciation rates through time estimated by ClaDS using the 28S
1286 large sub-unit of the rRNA gene (LSU rRNA gene).
1287 **Supplementary Figure 17:** Low support for extinction according to CoMET.
1288 **Supplementary Figure 18:** Inferred diversification rates decline faster in time-dependent
1289 models with fixed extinction rates.
1290 **Supplementary Figure 19:** Inferred diversification rates decline faster in congruent models
1291 with fixed extinction rates.

1292 **Supplementary Figure 20:** Variation of the environmental variables through time tested
1293 with RPANDA.

1294 **Supplementary Figure 21:** Speciation rates through time according to the temperature-
1295 dependent diversification model in RPANDA.

1296 **Supplementary Figure 22:** Temperature-dependent models are significantly supported in
1297 Glomeromycotina.

1298 **Supplementary Figure 23:** Temperature-dependent models are significantly supported in
1299 Glomeromycotina, even when using sampling fractions <90%.

1300 **Supplementary Figure 24:** Effect of the Glomeromycotina crown age on the RPANDA
1301 models.

1302 **Supplementary Figure 25:** Temperature-dependent models are not artifactually supported
1303 when time-dependency is simulated.

1304 **Supplementary Figure 26:** Temperature-dependent models are not supported because of
1305 a global temporal trend in temperature variation.

1306 **Supplementary Figure 27:** The support for temperature-dependent models is not linked to
1307 the heterogeneity of rates across lineages.

1308 **Supplementary Figure 28:** The different Glomeromycotina sub-clades present significant
1309 support for temperature-dependence diversification, but also for dependences with CO₂
1310 and land plants.

1311 **Supplementary Figure 29:** Diversification models estimated with RPANDA when using
1312 the 28S large sub-unit of the rRNA gene (LSU rRNA gene).

1313 **Supplementary Figure 30:** Characterizing Glomeromycotina niche width using principal
1314 coordinate analysis (PCA).

1315 **Supplementary Figure 31:** Characterizing Glomeromycotina niche width using principal
1316 coordinate analysis (PCA): Individual projection on the two principal coordinates
1317 according to the different Glomeromycotina delineations.

1318 **Supplementary Figure 32:** Characterizing Glomeromycotina niche width using principal
1319 coordinate analysis (PCA): Projection of the 10 abiotic and biotic variables on the two
1320 principal coordinates according to the different Glomeromycotina delineations.

1321 **Supplementary Figure 33:** Correlations between speciation rates at the tips, estimates of
1322 genetic diversity (Tajima's $\theta\pi$ estimator - referred to as "Nei diversity") and PC1 and
1323 PC2 coordinates.

1324 **Supplementary Figure 34:** The *Rhizophagus* clade with large niche width present the
1325 highest speciation rates.

1326 **Supplementary Figure 35:** Significant latitudinal gradient of Glomeromycotina diversity.

1327 **Supplementary Figure 36:** The total number of Glomeromycotina species is not higher in
1328 (tropical) grasslands.

1329 **Supplementary Figure 37:** No effect of ecosystem types or climatic zones on
1330 Glomeromycotina speciation rates.

1331 **Supplementary Figure 38:** No significant effect of mean spore length on VT speciation
1332 rates.

1333 **Supplementary Figure 39:** No significant correlation between mean spore length and
1334 endemism.

1335 **Supplementary Figure 40:** Average Glomeromycotina speciation rates and land plant
1336 diversity are decoupled for ~130 Myr.

1337